LEVEL II

SDAC-TR-79-3

(12)

EXPERIMENTAL SPECTRAL ANALYSIS OF SALMON/STERLING DECOUPLING

R.R. Blandford & J.R. Woolson
Seismic Data Analysis Center
Teledyne Geotech, 314 Montgomery Street, Alexandria Virginia 22314

30 November 1979

APPROVED FOR PUBLIC RELEASE: DISTRIBUTION UNLIMITED.

Sponsored by
The Defense Advanced Research Projects Agency (DARPA)
DARPA Order No. 2551

Monitored By
AFTAC/VSC
312 Montgomery Street, Alexandria, Virginia 22314

Disclaimer: Neither the Defense Advanced Research Projects Agency nor the Air Force Technical Applications Center will be responsible for information contained herein which has been supplied by other organizations or contractors, and this document is subject to later revision as may be necessary. The views and conclusions presented are those of the authors and should not be interpreted as necessarily representing the official policies, either expressed or implied, of the Defense Advanced Research Projects Agency, the Air Force Technical Applications Center, or the US Government.

Unclassified

SECURITY CLASSIFICATION OF THIS PAGE (When Data Entered)

REPORT DOCUMENTATION PAGE

READ INSTRUCTIONS BEFORE COMPLETING FORM

1. REPORT NUMBER: SDAC-TR-79-3
2. GOVT ACCESSION NO.: AD-A097 827
3. RECIPIENT'S CATALOG NUMBER:
4. TITLE (and Subtitle): EXPERIMENTAL SPECTRAL ANALYSIS OF SALMON/STERLING DECOUPLING
5. TYPE OF REPORT & PERIOD COVERED: Technical rept.
6. PERFORMING ORG. REPORT NUMBER:
7. AUTHOR(s): ~~R. R. Blandford~~ Robert R. Blandford, J. R. Woolson
8. CONTRACT OR GRANT NUMBER(s): F08606-79-C-0007, DARPA Order-2552
9. PERFORMING ORGANIZATION NAME AND ADDRESS: Teledyne Geotech, 314 Montgomery Street, Alexandria, Virginia 22314
10. PROGRAM ELEMENT, PROJECT, TASK AREA & WORK UNIT NUMBERS: VT/9709
11. CONTROLLING OFFICE NAME AND ADDRESS: Defense Advanced Research Projects Agency, Nuclear Monitoring Research Office, 1400 Wilson Blvd. Arlington, Virginia 22209
12. REPORT DATE: 30 November 1979
13. NUMBER OF PAGES: 60
14. MONITORING AGENCY NAME & ADDRESS (if different from Controlling Office): VELA Seismological Center, 312 Montgomery Street, Alexandria, Virginia 22314
15. SECURITY CLASS. (of this report): Unclassified
15a. DECLASSIFICATION/DOWNGRADING SCHEDULE:

16. DISTRIBUTION STATEMENT (of this Report)

APPROVED FOR PUBLIC RELEASE; DISTRIBUTION UNLIMITED.

17. DISTRIBUTION STATEMENT (of the abstract entered in Block 20, if different from Report)

18. SUPPLEMENTARY NOTES

19. KEY WORDS (Continue on reverse side if necessary and identify by block number)

Salmon
Sterling
Decoupling

20. ABSTRACT (Continue on reverse side if necessary and identify by block number)

Re-analysis of SALMON and STERLING initial short-period compressional and surface waves at station PLMS (Poplarville, Mississippi) at a distance of 27 km shows a SALMON/STERLING compressional phase spectral ratio tending to a ratio of only 17 at 25 Hz in agreement with the theoretical calculations of Patterson (1966) and of Healy, King, and O'Neill (1971). The spectral ratio for the surface waves tends to a ratio of approximately 100 at 25 Hz, in agreement with spectral ratios previously reported by Springer, Denny, Healy, and Mickey (1968), whose data window at PLMS was large enough to

over page

DD FORM 1 JAN 73 1473 EDITION OF 1 NOV 65 IS OBSOLETE

Unclassified 408258

SECURITY CLASSIFICATION OF THIS PAGE (When Data Entered)

consist predominantly of surface waves. The fact that the ratio varies as a function of phase suggests that decoupling varies as a function of take-off angle, with the least decoupling occurring at high frequencies for the most steeply departing rays.

Another topic discussed is the apparent variation in decoupling as defined by the ratio of STERLING/STERLING HE. The variation in this ratio is determined to be explainable by the variation in shot point between these two explosions, and not necessarily by a variation in decoupling as a function of azimuth.

EXPERIMENTAL SPECTRAL ANALYSIS OF SALMON/STERLING DECOUPLING

SEISMIC DATA ANALYSIS CENTER REPORT NO.: SDAC-TR-79-3

AFTAC Project Authorization No.: VELA T/9709/B/ETR

Project Title: Seismic Data Analysis Center

ARPA Order No.: 2551

Name of Contractor: TELEDYNE GEOTECH

Contract No.: F08606-79-C-0007

Date of Contract: 01 October 1979

Amount of Contract: $279,929

Contract Expiration Date: 30 September 1980

Project Manager: Robert R. Blandford
(703) 836-3882

P.O. Box 334, Alexandria, Virginia 22313

ABSTRACT

Re-analysis of SALMON and STERLING initial short-period compressional and surface waves at station PLMS (Poplarville, Mississippi) at a distance of 27 km shows a SALMON/STERLING compressional phase spectral ratio tending to a ratio of only 17 at 25 Hz, in agreement with the theoretical calculations of Patterson (1966) and of Healy, King, and O'Neill (1971). The spectral ratio for the surface waves tends to a ratio of approximately 100 at 25 Hz, in agreement with spectral ratios previously reported by Springer, Denny, Healy, and Mickey (1968), whose data window at PLMS was large enough to consist predominantly of surface waves. The fact that the ratio varies as a function of phase suggests that decoupling varies as a function of take-off angle, with the least decoupling occurring at high frequencies for the most steeply departing rays.

Another topic discussed is the apparent variation in decoupling as defined by the ratio of STERLING/STERLING HE. The variation in this ratio is determined to be explainable by the variation in shot point between these two explosions, and not necessarily by a variation in decoupling as a function of azimuth.

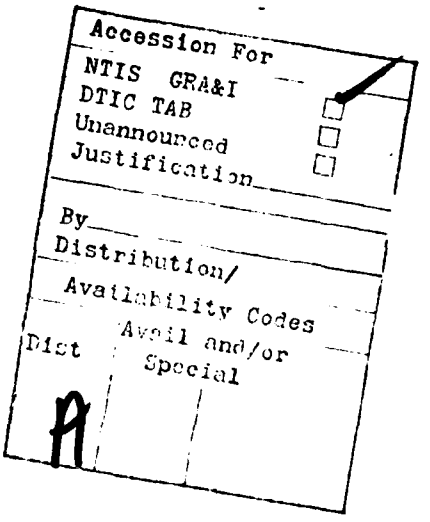

TABLE OF CONTENTS

LIST OF FIGURES

LIST OF FIGURES (Continued)

LIST OF FIGURES (Continued)

LIST OF FIGURES (Continued)

LIST OF FIGURES (Continued)

INTRODUCTION

The 5.3 ± 0.5 kiloton (Werth and Randolph, 1966) explosion SALMON was detonated at 1600 GMT on October 22, 1964 at a depth of 827.8 meters at location 31.1421°N, 89.5701°W. The shot created a stable cavity of approximate radius 17 meters. At 1215 GMT on December 3, 1966 the 0.38 kiloton explosion STERLING was detonated at the center of this cavity. The purpose of this experiment was to test the theory of decoupling; that the seismic signals of the smaller explosion would be smaller than they would have been without the large cavity.

Figures 1 and 2 show relevant details of the shots' environment. Further details on SALMON may be found in a special edition of the Journal of Geophysical Research containing a lead article by Werth and Randolph (1966).

Springer et al.(1968) (hereafter referred to as SDHM) produced a paper comparing the results of the experiment to the predictions of theory, as did Murphy (1969) and Healy et al. (1971). Although each of these authors noted that the decoupling efficiency decreased with increasing frequency on both theoretical and experimental grounds, this fact did not receive a great deal of attention because if results were scaled to yields of interest, the frequencies of less efficient decoupling lay in the range 3-10 Hz, generally beyond the range of detectibility for teleseismic observations.

However, in recent years the possibility has arisen that observations may be allowed within the USSR at regional distances from salt deposits where evasion of a comprehensive test ban treaty might be attempted by means of decoupling in salt.

Werth, G. and P. Randolph (1966). The SALMON seismic experiment, J. Geophys. Res, 71, 3405-3414.

Springer, D., M. Denny, J. Healy, and W. Mickey (1968). The STERLING experiment: decoupling of seismic waves by a shot-generated cavity, J. Geophys. Res., 73, 5995-6011.

Murphy, J. R. (1969). Discussion of paper by D. Springer, J. Healy, M. Denny, and W. Mickey, The STERLING experiment: decoupling of seismic waves by shot-generated cavity, J. Geophys. Res., 74, 6714-6718.

Healy, J. H., C. King and M. E. O'Neill (1971). Source parameters of the SALMON and STERLING nuclear explosions from seismic measurements, J. Geophys. Res., 76, 3344-3355.

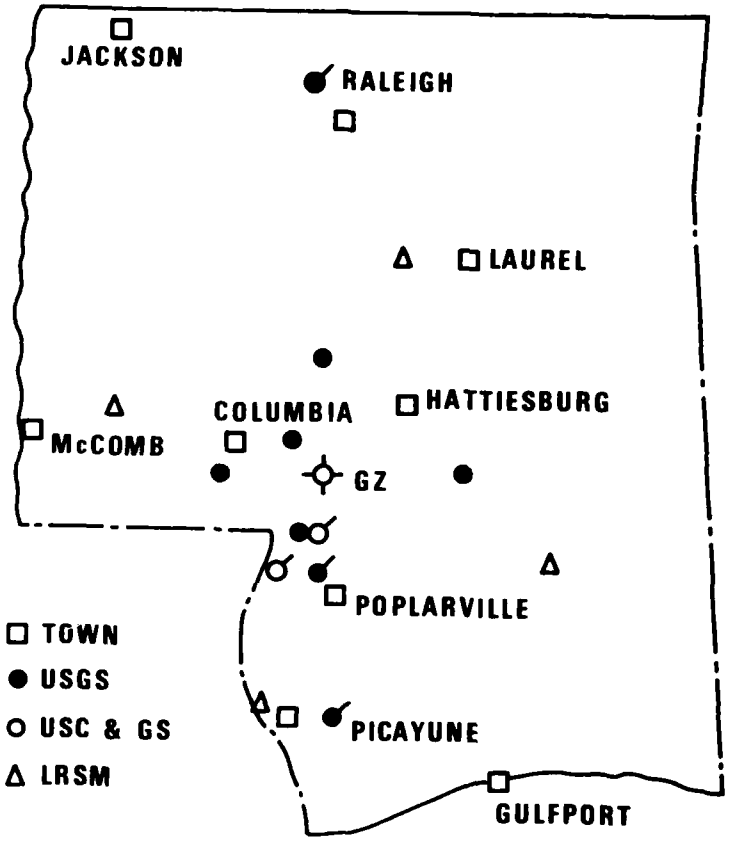

Figure 1. Location of seismic recording stations observing signals from STERLING. Flagged locations also recorded SALMON (from Springer et al., 1969).

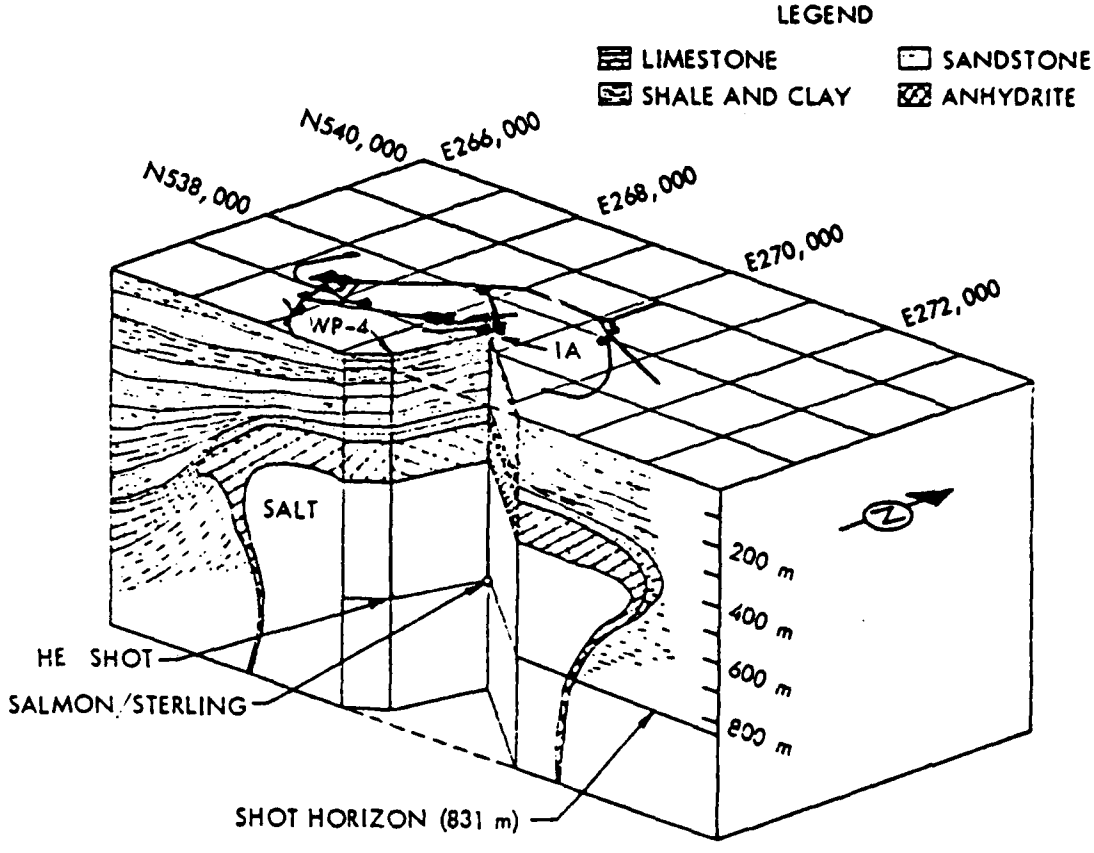

Figure 2. Source locations of STERLING nuclear and HE shots (from Springer et al., 1968).

So important is this point that it seems to justify a re-examination of the original raw data to see if a more critical examination than was originally justified of the signals at high frequencies might not give some fresh insights to the problem.

Characteristics of the Data

In Figure 1 we see a plan view of the stations recording the STERLING event. We see that five stations recorded both SALMON and STERLING. The three United States Geological Survey (USGS) stations were at Rayleigh, Poplarville, and Picayune; we refer to them in this report as stations RLMS, PLMS, and PYMS, respectively. The station distances are 112, 27 and 69 kilometers, respectively. Through the courtesy of J. Healy and M. O'Neill of the USGS, we received the original field analog tapes for these two events. We made an analog copy of all six tapes (one for each event at each station) and then digitized the copy at 100 samples per second.

Two other stations also recorded data from both SALMON and STERLING as indicated by the flagged open circles in Figure 1. These are the USC&GS stations 10-South and 20-South at distances of 16 and 32 kilometers, respectively. As of the writing of this report, we have found that this data is available from John Blume Associates in Las Vegas, Nevada; care of Mr. Jerry Kralik, and we have sent an analog tape to him requesting that he copy the original onto it.

Figure 2 shows a cross-section of the salt dome in which the explosions were detonated. Also shown in this view is the shot point for the high explosive shot referred to later in this report as the STERLING CAL or STERLING HE shot.

Figure 3 shows response curves for the systems which recorded data presented in this report. The LRSM response is displacement whereas the USGS and USC&GS responses are velocity. Figure 4 is the USGS displacement response and we see that it peaks at approximately 30 Hz. We shall see in this report that an even sharper high-frequency response should have been installed in order to keep the high-frequency portion of the SALMON signal above system noise at PLMS, RLMS and PYMS.

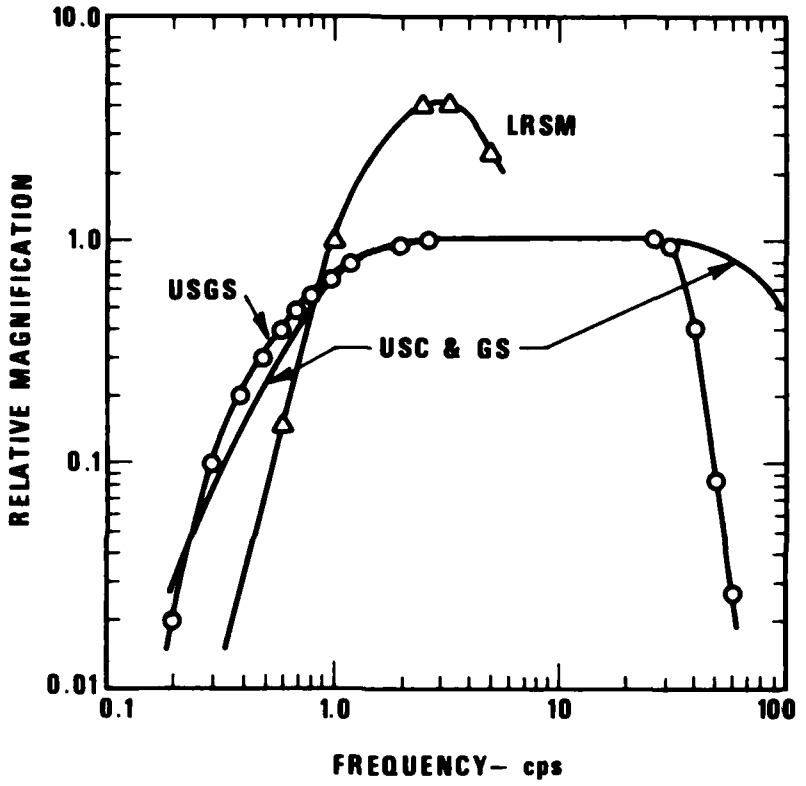

Figure 3. Relative response of the three recording systems. The Geotech system is displacement response, whereas the two broadband systems are calibrated to velocity sensitivity (from Springer et al., 1968).

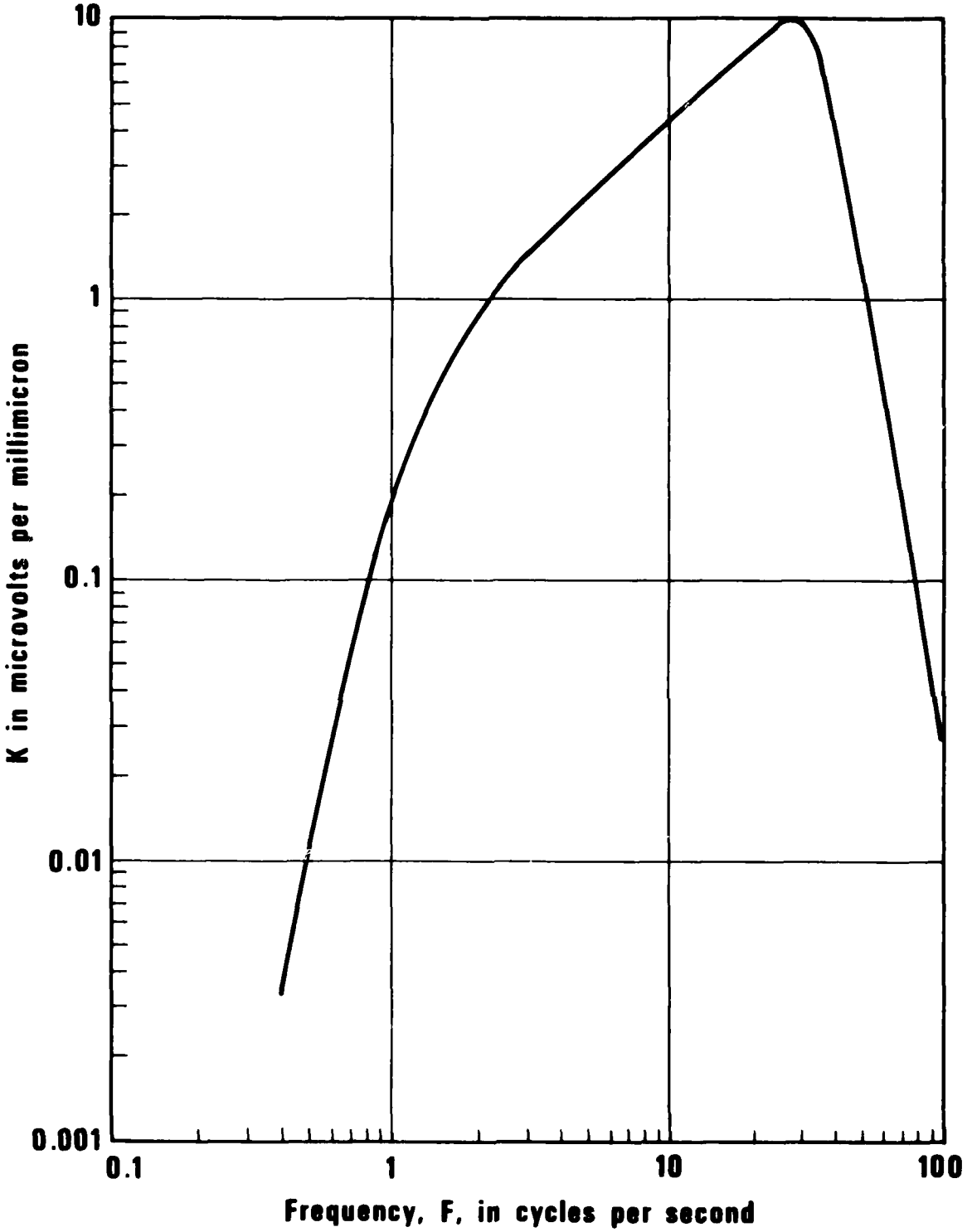

Figure 4. Displacement response of the recording system used to record SALMON and STERLING (from Borcherdt et al., 1967).

In Figure 5 we see the raw data and calibrations at PLMS, the most crucial station. SDHM point out that channels 2 and 5 should not be used for comparison of SALMON and STERLING because different instruments were used on these channels for SALMON. Inspection of figures in the field report of Borcherdt et al. (1967) indeed shows that these channels have high-frequency noise in front of the signal.

When we plotted out the SALMON P wave signals for PLMS, channels 4 and 6, we noted several data spikes. Upon re-examination of the Borcherdt et al. (1967) plots we noted that these spikes were also visible. The effects of these spikes may be seen in the SALMON signal spectra presented by Borcherdt et al. (1967). Since these spikes will result in a high high-frequency signal level (leading to an overestimate of decoupling efficiency) we have chosen not to analyze these channels. This leaves only channels 1 and 3 at PLMS.

In a broad-band sense we see from Figure 5 that the spectral ratio for $f \leq 10$ Hz is approximately 1000. From Figure 6 it is apparent that STERLING has proportionally more high-frequency than does SALMON. We can see also in Figure 6 that at low frequencies SALMON and STERLING have similar waveforms whereas HE is different. This is presumably a propagation effect.

Figure 7 from station 10-south shows the same qualitative features as does PLMS, and emphasizes the importance of acquiring these data.

Figure 8 shows the average spectral ratio determined by SHDM. For reasons to be discussed later in this report, we believe that the ratio of approximately 100 at 20 Hz is too large. One reason for this may be the spikes on channels 4 and 6 noted above. Another is the fact, as we shall show, that at least in the data as we see it now for SALMON, only channel 1 of PLMS has S/N > 1.0 for f > 12 Hz. At stations RLMS and PYMS for SALMON no channel has S/N > 1 for f > 12 Hz. Thus the ratio seen in Figure 8 would be biased upward for f > 12 Hz. Finally, another source of bias is the fact, which we will see, that the surface waves show more efficient decoupling at high frequencies than do the compressional waves. Assuming that the compressional waves are of principal interest, the fact that the window used by Borcherdt et al. (1967) from which SDHM took their data was 12 seconds long and at

---

Borcherdt, R. D., J. H. Healy, W. H. Jackson and D. H. Warren (1967). Seismic measurements of explosions in the Tatum salt dome, Mississippi Technical Letter Number 48, United States Geological Survey.

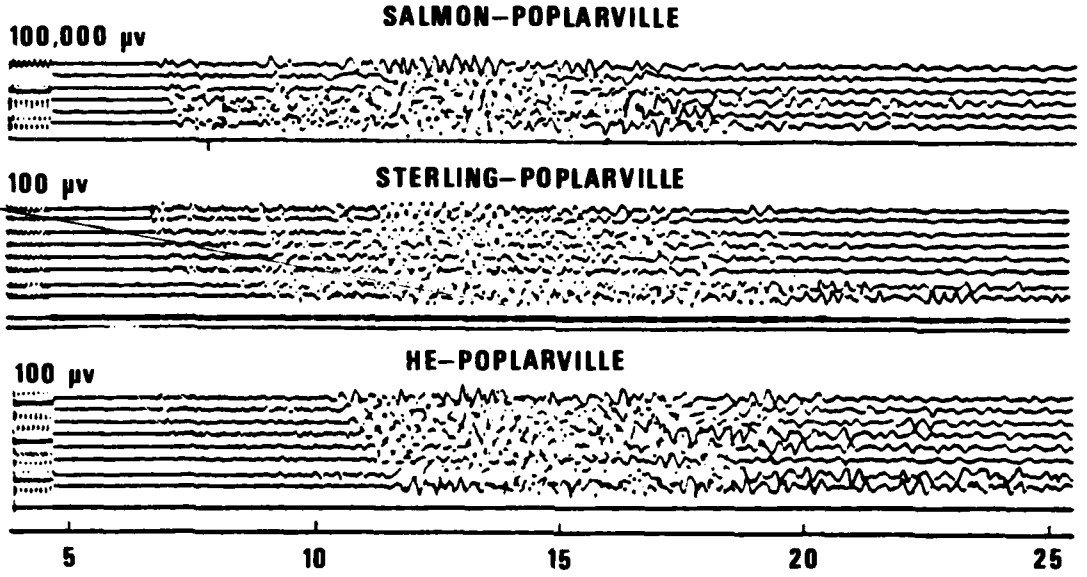

Figure 5. Sample broadband recordings made by the USGS at Poplarville. Calibration signals are shown at the left of each trace. The relative magnification to SALMON of trace 1 for STERLING is about 690 and for HE is 1250. SALMON traces 2 and 5 are from different instruments, which were not duplicated on STERLING. Traces 7 and 8 of the STERLING and HE records are from horizontal component seismometers (from Springer et al., 1968).

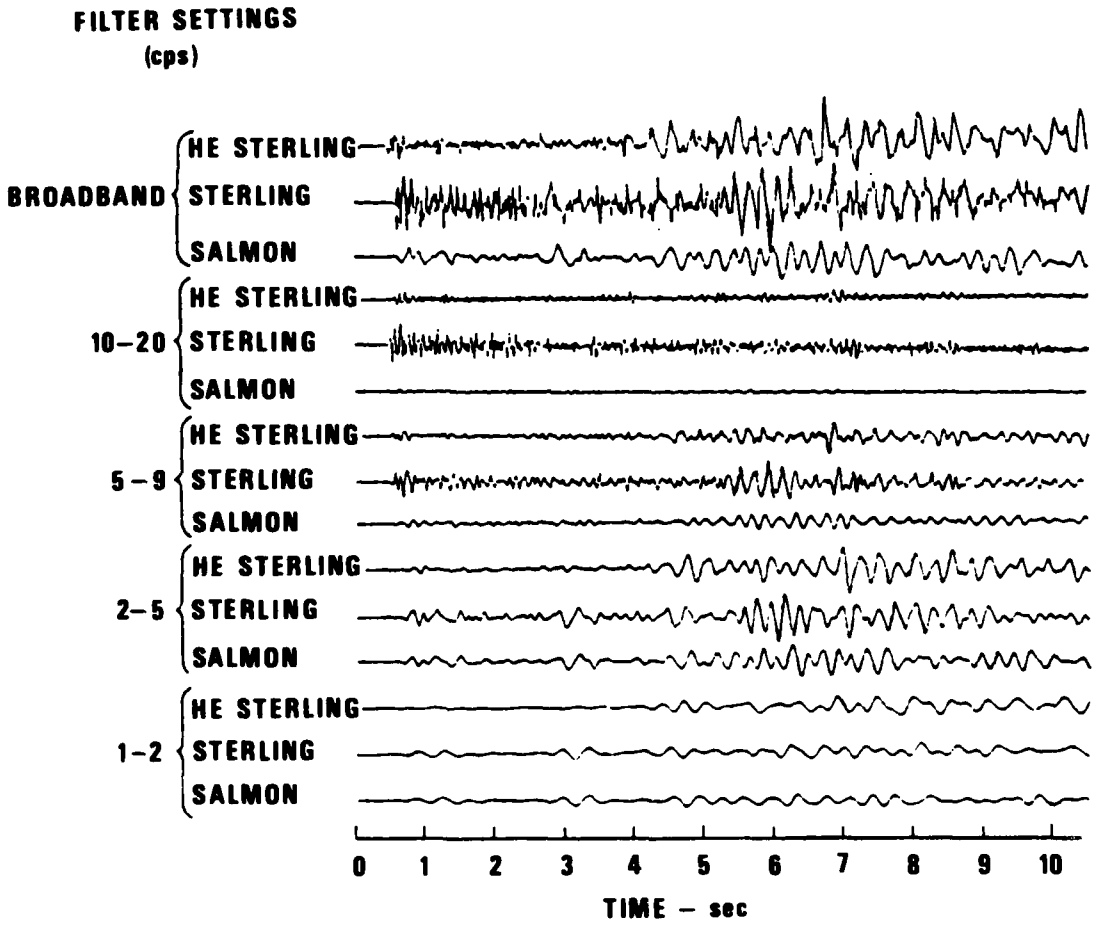

Figure 6. Comparison of SALMON, STERLING, and HE analog playbacks in different frequency bands. For illustration, the magnifications have been adjusted to give approximately the same amplitudes (from Springer et al., 1968). Signals at Poplarville.

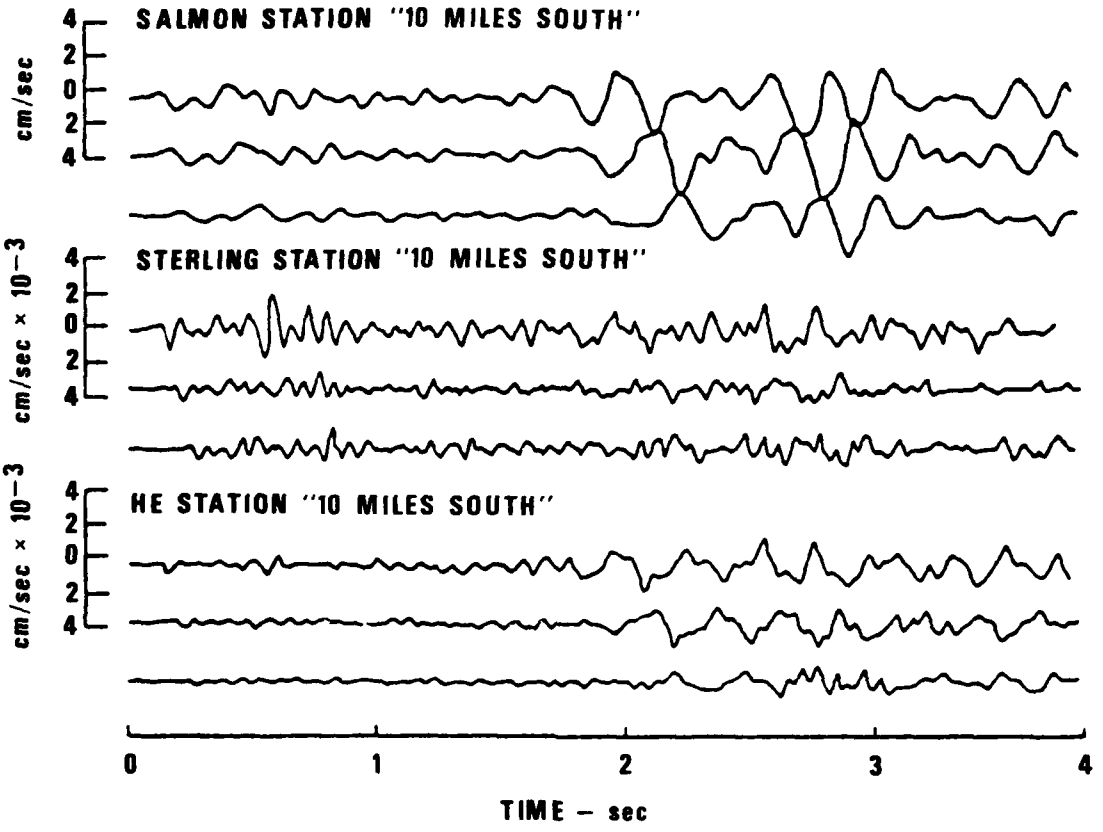

Figure 7. Sample broadband recordings of SALMON, STERLING and HE, vertical, radial and transverse made by the USGS at a station 16 km south of SALMON. The relative magnification is shown in the traces (from Springer et al., 1968).

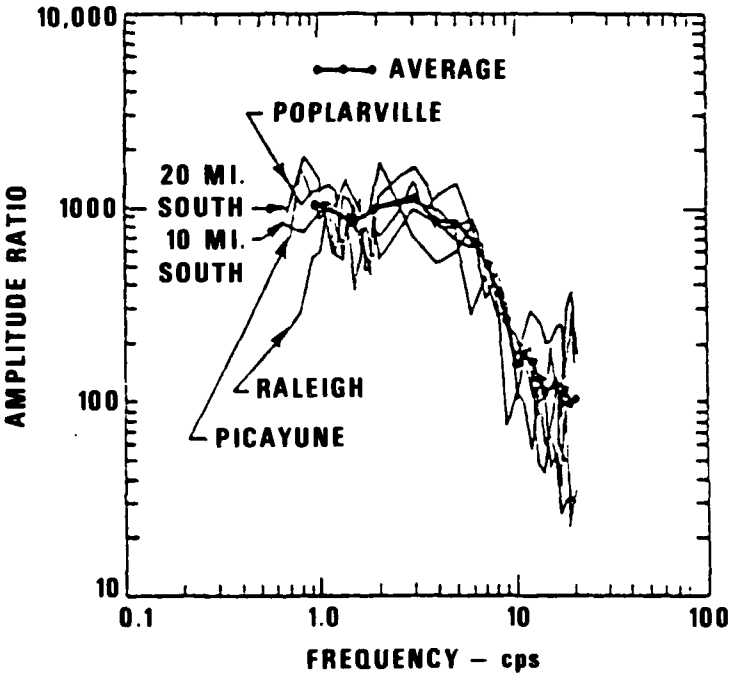

Figure 8. Ratio of SALMON spectra to STERLING spectra. The ratios shown for a station are the average for that station. The solid line is the smoothed average of all five station averages (from Springer et al., 1968).

PLMS, 10S, and 20S included surface waves, will have biased the ratio from that appropriate for compressional waves.

To establish the calibrations for these data we have used the microvolts per millimicron scale on Figure 4 from Borcherdt et al. (1967), and have assumed that the high amplitude 10 Hz calibration signals which we digitized from the analog tape had the amplitudes in microvolts as indicated on plots similar to Figure 5 which we found in Borcherdt et al. (1967). We had to rely on these plots rather than original field logs because government sources have told us that these logs are difficult to retrieve from government storage.

For consistency with standard teleseismic regional practice the time series and spectral amplitudes are reported relative to 1 Hz even though the calibration frequency is at 10 Hz. To obtain true ground motion at any frequency divide by the relative response as seen in Figure 4 between the observed frequency and 1 Hz.

ANALYSIS OF SALMON/STERLING SPECTRAL RATIO AT POPLARVILLE, RAYLEIGH, PICAYUNE

Figure 9a shows the most crucial data available relevant to the question of SALMON/STERLING decoupling. The first trace is 2.5 seconds of the noise in front of the signal. As can be seen, a 10% cosine taper has been applied to the data, and the resulting amplitude spectrum is seen below in the logarithmic plot as a dotted line. We note that the noise is dominated by peaks at 1, 12, and 25 Hz.

The second trace in Figure 9a is the initial P signal from SALMON, tapered in the same way as the noise. The spectrum is seen below in logarithmic and linear amplitude plots as a solid line. We see that S/N > 1 from 0.5 Hz to 23 Hz, and possibly in a small interval from 30 Hz to 33 Hz.

Figure 9b is the same as Figure 9a except that it is from channel 3 which, as we saw above, is the only channel besides channel 1 which we may use at PLMS for a spectral ratio between SALMON and STERLING. Comparing the plots, we see that the noise in the 12 to 20 Hz band is much higher for channel 3 than for channel 1. This is, of course, immediately apparent by comparison of the raw noise waveforms. In apparent disagreement with this, the noise spectra presented by Borcherdt et al. (1967) show much greater noise on channel 1; however, the nature of their channel 1 noise spectrum is that of a spike or step in the data, suggesting that some error crept into the data processing. In the Borcherdt et al. (1967) signal spectra for channels 1 and 3, we see an increased high-frequency level on channel 3, which in our analysis we trace to the increased high-frequency noise.

In any event, our analysis suggests that channel 3 adds no information to the spectral ratio beyond 12 Hz and so we shall ignore it in subsequent analysis, leaving the analysis to rest completely on the channel 1 data.

In Figure 10 we see the noise and signal waveforms and spectra for STERLING P wave at PLMS. If one overlays the SALMON and STERLING signals, it is easy to see that SALMON is similar to a low-passed version of STERLING. This is also suggested by the spectra: one sees in the logarithmic plot that the heavy solid line, which is the SALMON spectrum plotted at a scale of 1/1000, closely parallels the STERLING spectrum up to 4 Hz, where it then

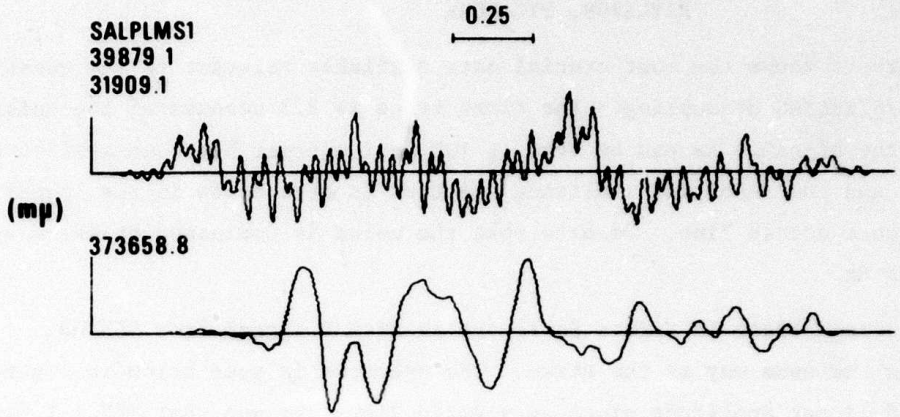

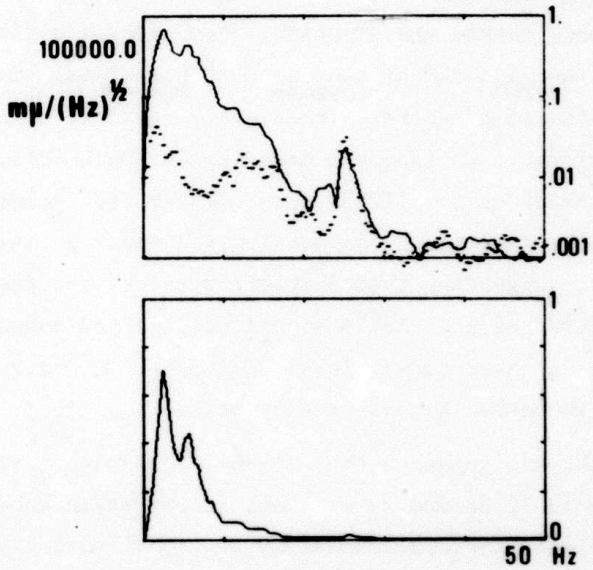

Salmon P wave signal and noise at PLMS. (Channel 1)

Figure 9a. Upper trace is noise in front of signal, lower trace is signal. Units of millimicrons at 1.0 Hz. Data sampled at 100 sps. Upper spectrum is square root of power spectrum with units millimicrons/$(Hz)^{1/2}$. Solid line is signals, dashed line is noise. Lower spectrum is the same except with a linear rather than logarithmic vertical scale, and without the noise spectrum.

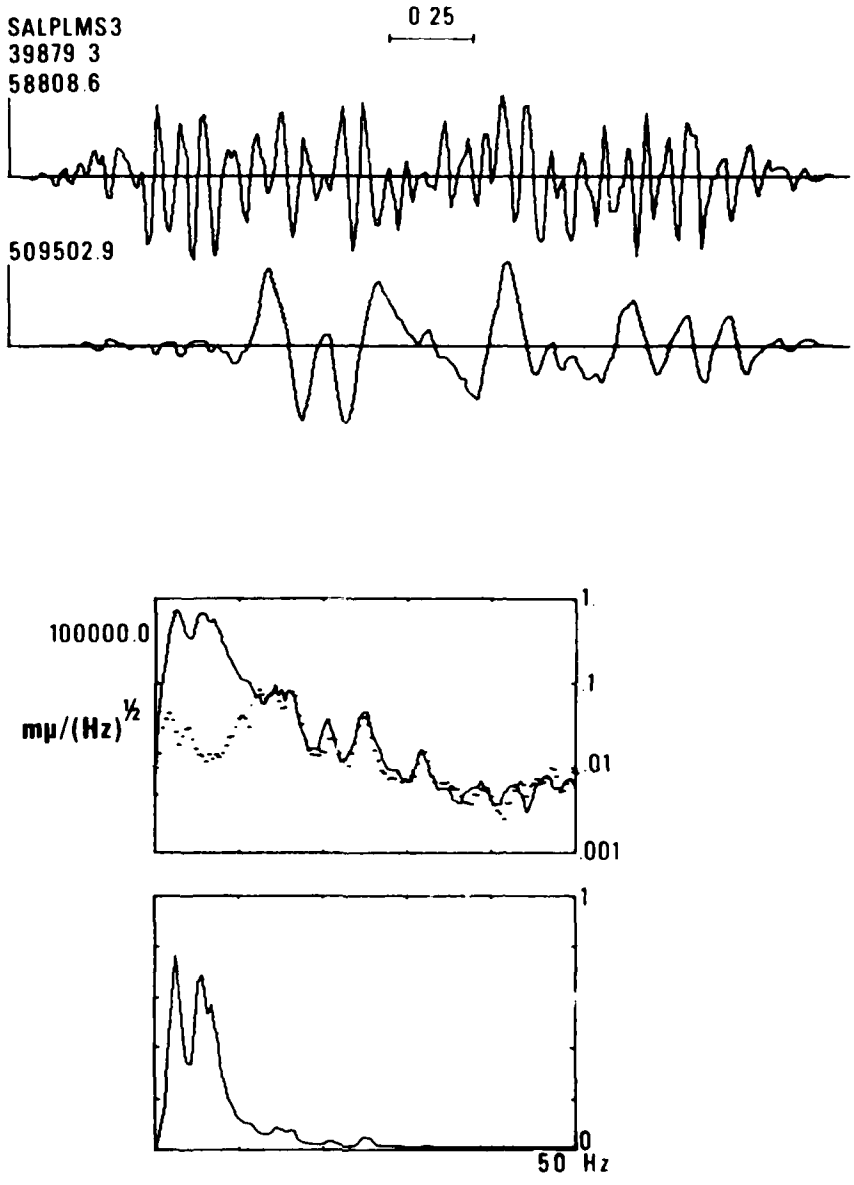

Salmon P wave signal and noise at PLMS. (Channel 3)

Figure 9b. Upper trace is noise in front of signal, lower trace is signal. Units of millimicrons at 1.0 Hz. Data sampled at 100 sps. Upper spectrum is square root of power spectrum with units millimicrons/$(Hz)^{1/2}$. Solid line is signals, dashed line is noise. Lower spectrum is the same except with a linear rather than logarithmic vertical scale, and without the noise spectrum.

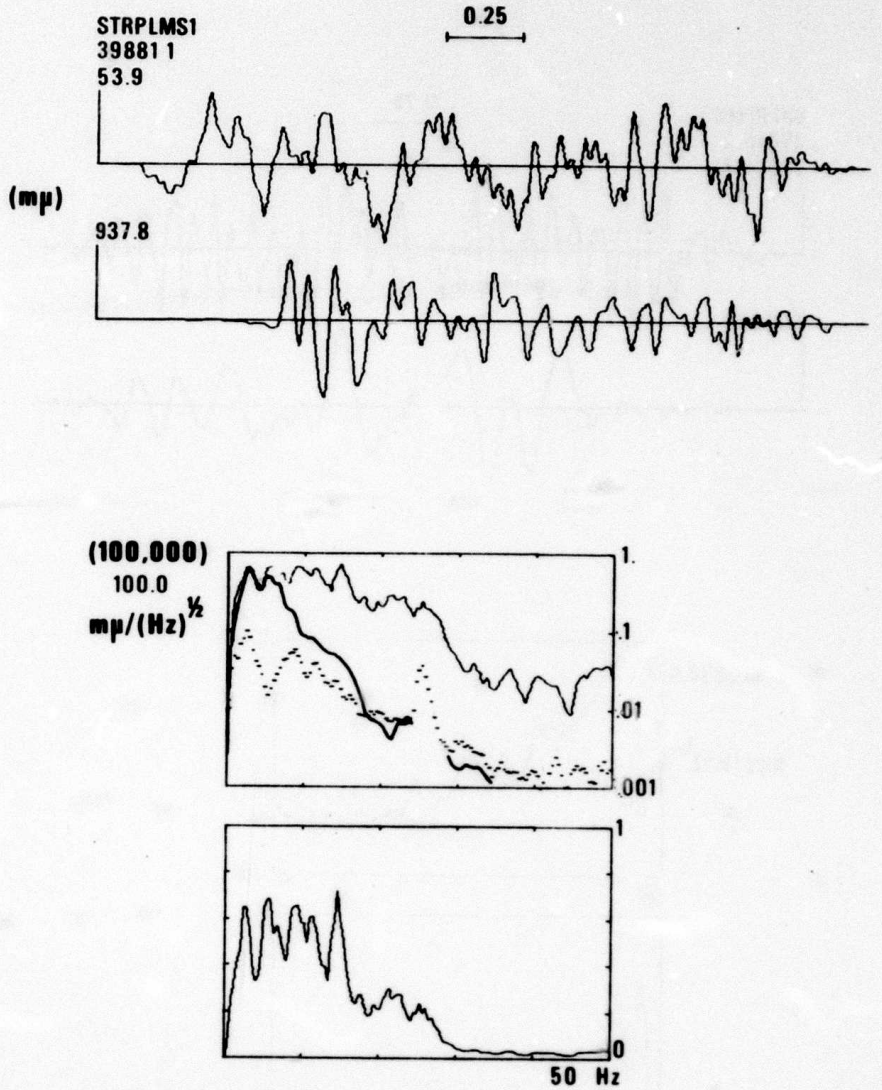

Sterling P wave signal and noise at PLMS.

Figure 10. Upper trace is noise in front of signal, lower trace is signal. Units of millimicrons at 1.0 Hz. Data sampled at 100 sps. Upper spectrum is square root of power spectrum with units millimicrons/$(Hz)^{1/2}$. Solid line is signal, dashed line is noise. Lower spectrum is the same except with a linear rather than logarithmic vertical scale, and without the noise spectrum channel 1. The maximum amplitude in parentheses is appropriate for the SALMON spectrum.

departs. (This, of course, immediately suggests that the corner frequency for SALMON is in the neighborhood of 4 Hz.)

The space between the two solid lines in Figure 10 represents the spectral ratio between SALMON and STERLING, and will be used in subsequent figures.

Figures 11 and 12 are analogous to Figures 9a and 10 except that they are for the surface wave or "L_g" signal, and utilize a 5-second instead of a 2.5 second window. In both the time and spectral domains, we can see that there is not as much extra high-frequency in STERLING for L_g as there was for P, showing that at high frequencies the decoupling is more efficient for L_g than for P. (This is obviously not an attenuation effect, since for every phase both paths are the same and attenuation cancels out.)

It seems well worth remarking that for STERLING, S/N >> 1 for both phases all the way to 50 Hz; but for SALMON, which had amplitudes 10-1000 times greater, S/N > 1.0 only for f < 12 Hz. This is due to the more rapid fall-off of the SALMON source spectrum which, as a result, dips below the system noise. If the SALMON experiment were to be repeated it would be necessary either to use a system with greater dynamic range or to peak the system more sharply.

Figure 13 and 14 are analogous to Figures 9a and 10 except that they are for the station RLMS at a distance of 112 km. Even at this distance note that the STERLING signal is well above the noise from 2 to 50 Hz, whereas SALMON again dips into the system noise. In Figure 14 we see that the heavy "SALMON" spectral line lies slightly below the STERLING spectrum. For the L_g window we see the same amplitude ratio. For L_g, however, S/N > 1 only for f < 5 Hz. There is much more high frequency in the STERLING P wave relative to SALMON P than high frequency in the STERLING L_g relative to SALMON L_g...just as for PLMS.

We have not presented the data from PYMS because suitable calibrations were not produced in the A/D process; however, examination of the signal and noise spectra shows that the situation is very similar to that at RLMS, i.e., the SALMON signal is lost in system noise around 12 Hz.

Figure 15 summarizes the data analysis. The solid lines have been produced by drawing smooth cuves through the data in Figures 10 and 12, picking off representative differences between the curves and plotting them in Figure 15. Then the curves are drawn in by hand. The stars are taken from

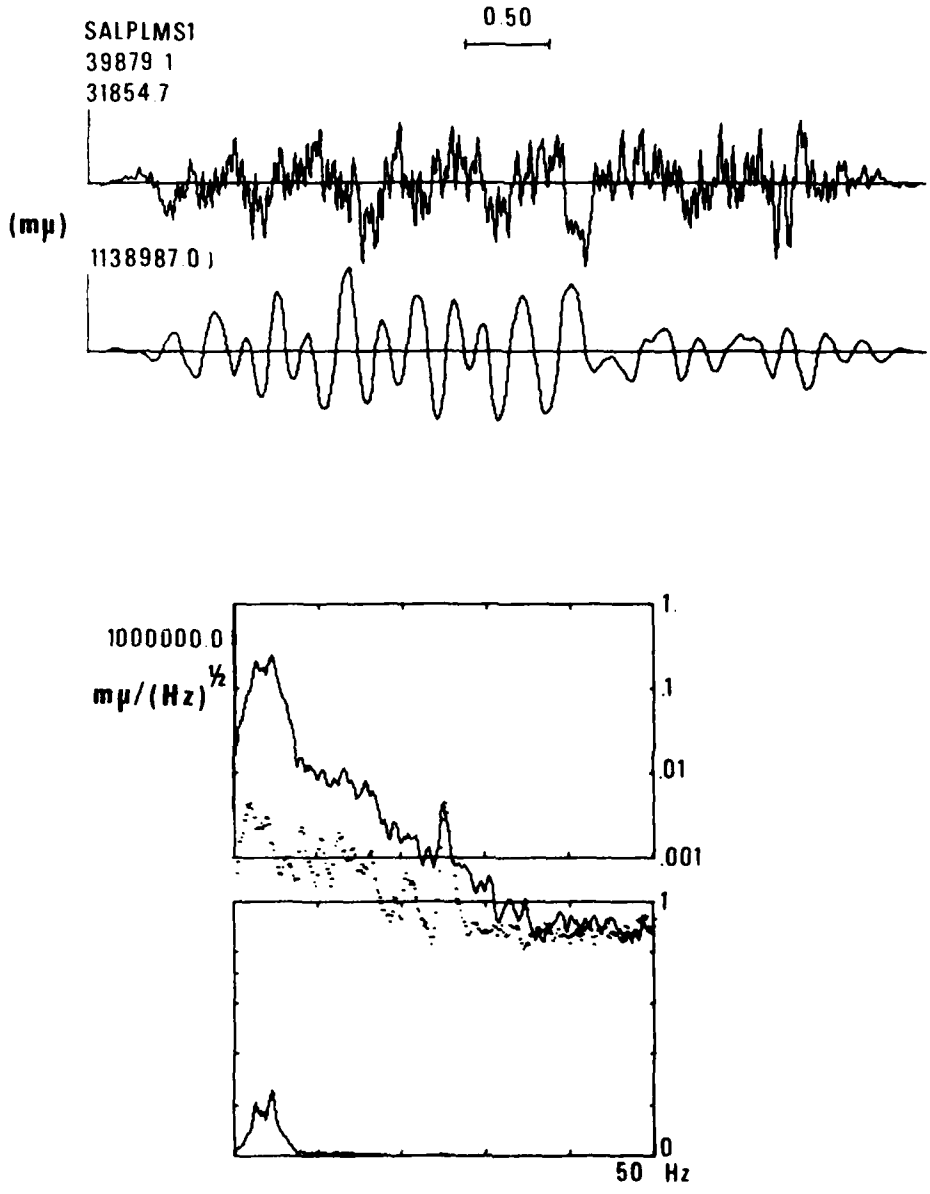

Salmon "Lg" signal and noise at PLMS.

Figure 11. Upper trace is noise in front of singal, lower trace is signal. Units of millimicrons at 1.0 Hz. Data sampled at 100 sps. Upper spectrum is square root of power spectrum with units millimicrons/(Hz) $^{1/2}$. Solid line is signal, dashed line is noise. Lower spectrum is the same except with a linear rather than logarithmic vertical scale, and without the noise spectrum channel 1.

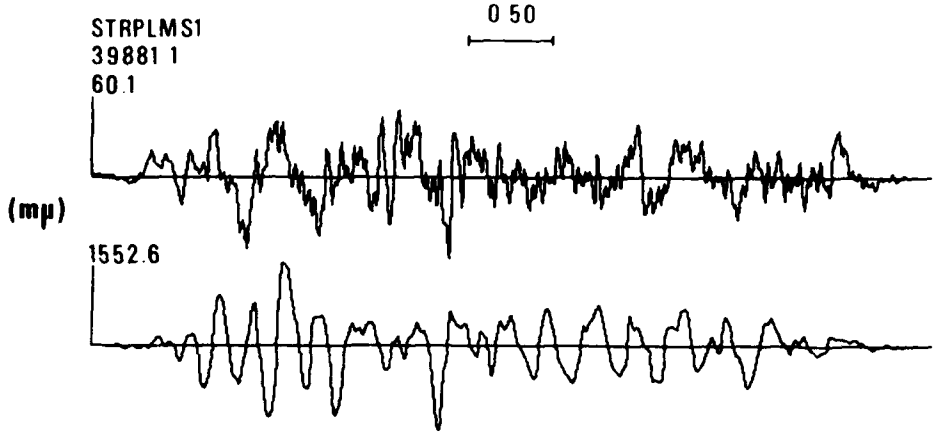

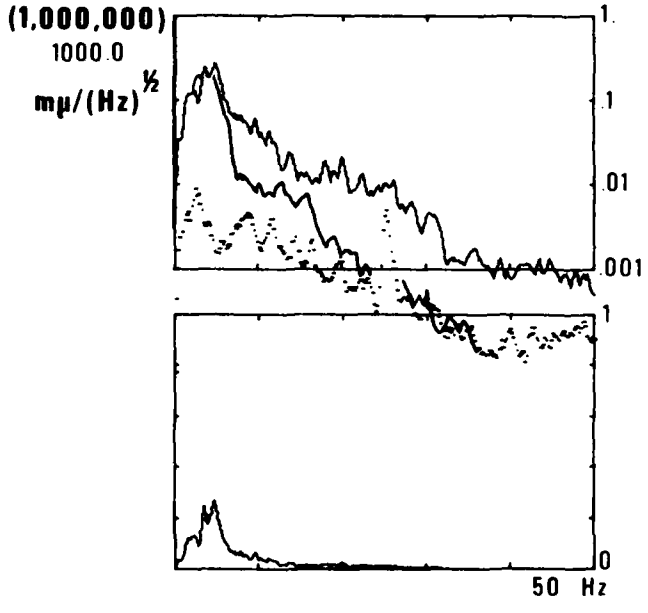

Sterling "Lg" signal and noise at PLMS.

Figure 12. Upper trace is noise in front of signal, lower trace is signal. Units of millimicrons at 1.0 Hz. Data sampled at 100 sps. Upper spectrum is square root of power spectrum with units millimicrons/(Hz) $^{1/2}$. Solid line is signal, dashed line is noise. Lower spectrum is the same except with a linear rather than logarithmic vertical scale, and without the noise spectrum channel. Heavy solid line on logarithmic plot is taken from the previous plot for SALMON where S/N = 1.0. The maximum amplitude in parentheses is appropriate for the SALMON spectrum.

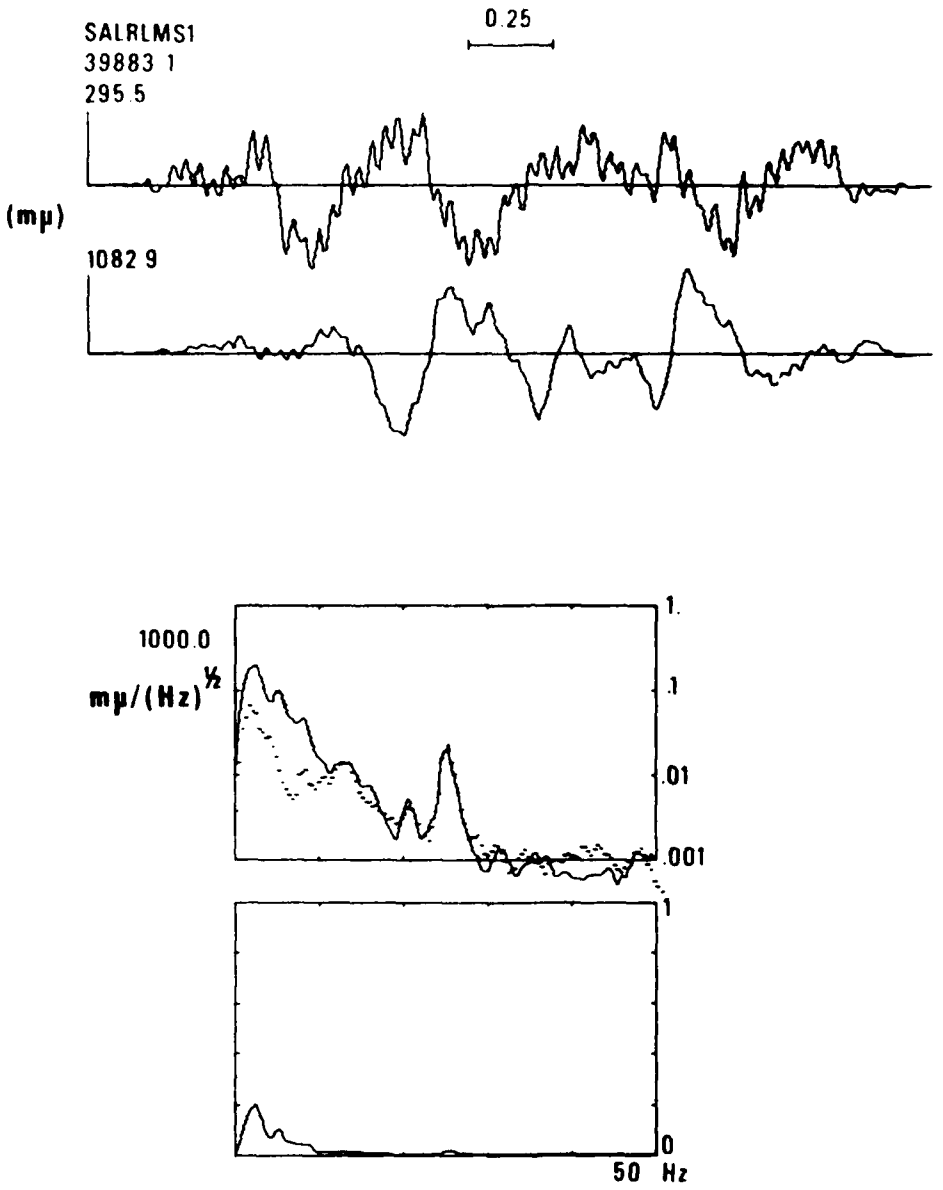

Salmon P wave signal and noise at RLMS.

Figure 13. Upper trace is noise in front of signal, lower trace is signal. Units of millimicrons at 1.0 Hz. Data sampled at 100 sps. Upper spectrum is square root of power spectrum with units millimicrons/(hz) 1/2. Solid line is signal, dashed line is noise. Lower spectrum is the same except with a linear rather than logarithmic vertical scale, and without the noise spectrum channel 1.

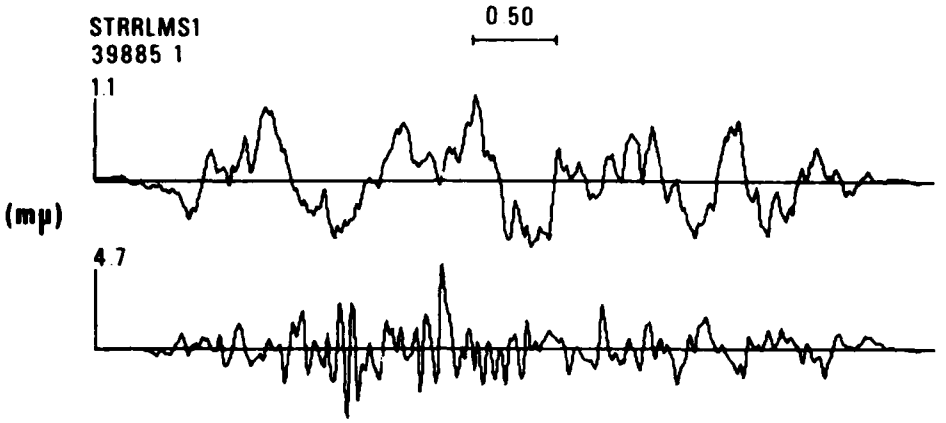

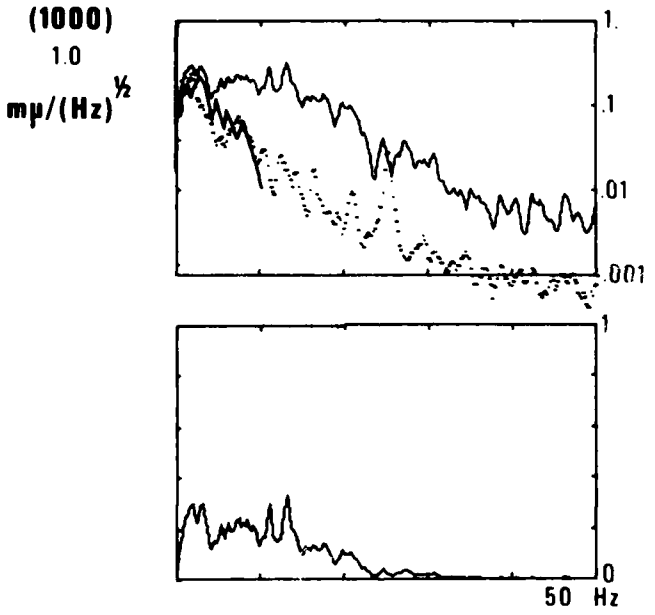

Sterling P wave signal and noise at RLMS.

Figure 14. Upper trace is noise in front of signal, lower trace is signal. Units of millimicrons at 1.0 Hz. Data sampled at 100 sps. Upper spectrum is square root of power spectrum with units millimicrons/(Hz) $^{1/2}$. Solid line is signal, dashed line is noise. Lower spectrum is the same except with a linear rather than logarithmic vertical scale, and without the noise spectrum channel 1. Heavy solid line on logarithmic plot is taken from the previous plot for SALMON where S/N > 1.0. The maximum amplitude in parentheses is appropriate for the SALMON spectrum.

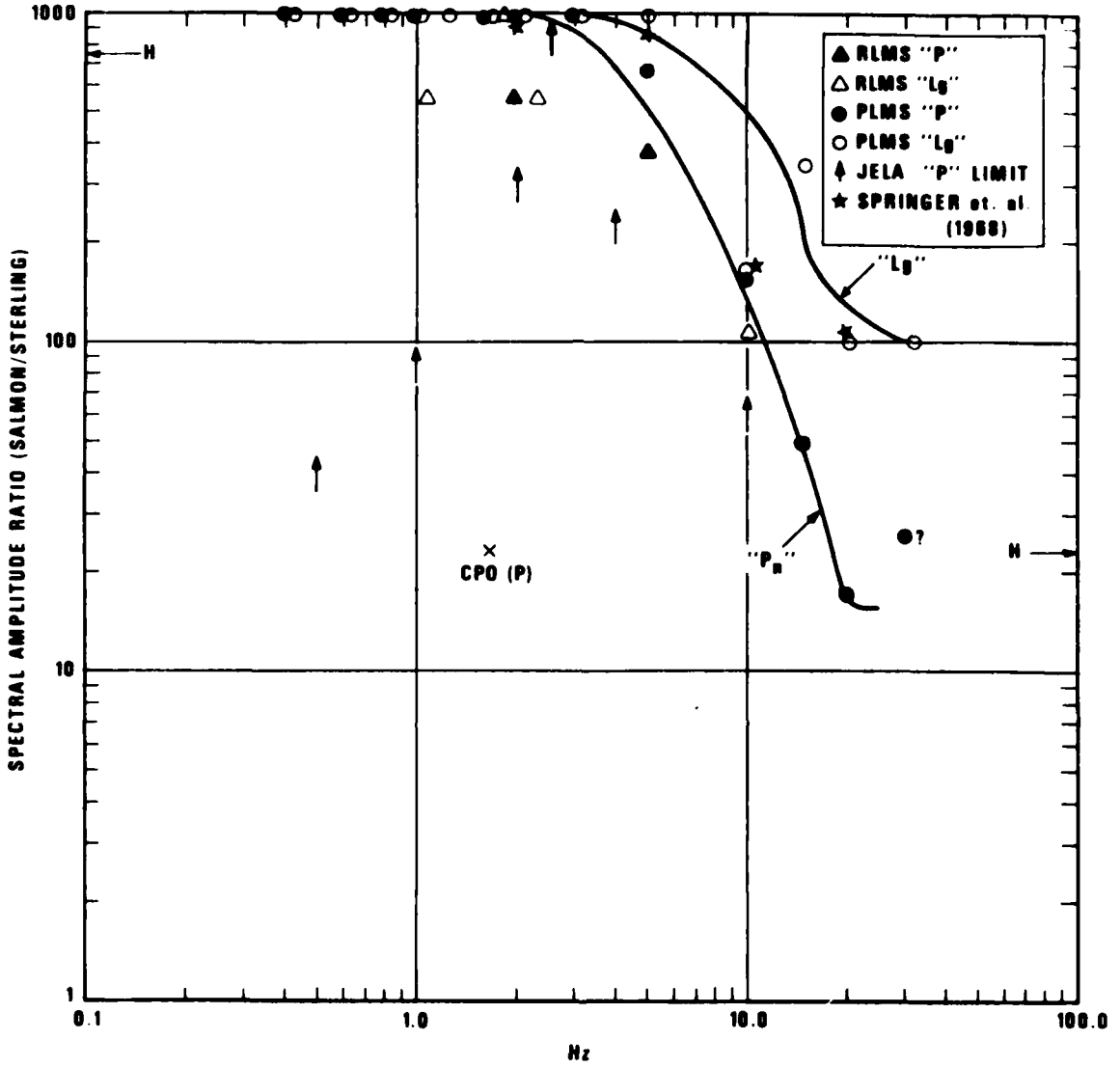

Figure 15. Spectral amplitude ratio of SALMON/STERLING, as seen for the P and "Lg" signals at PLMS and RLMS, all at channel 1. Arrows indicate lower limit for this ratio determined from the ratio of SALMON signal to the noise at the time of STERLING as determined at station JELA, and the X represents a similar measurement as made at CPO. The "H" symbols give the low and high frequency limits determined from "Sharpe" models fitted by Healy et al. (1971).

SDHM from the figure reproduced in our Figure 8. The vertical arrows represent a SALMON signal to STERLING noise spectral limit at JELA at Δ = 243 km which is discussed in more detail later in this report. The single CPO point was derived by measuring the period of the maximum P-wave film amplitude for SALMON, and then finding the largest noise pulse of that period in a

SDHM from the figure reproduced in our Figure 8. The vertical arrows represent a SALMON signal to STERLING noise spectral limit at JELA at Δ = 243 km which is discussed in more detail later in this report. The single CPO point was derived by measuring the period of the maximum P-wave film amplitude for SALMON, and then finding the largest noise pulse of that period in a -5, +30 second window around the expected STERLING arrival time.

We see that the JELA and CPO limits do lie below the observed ratios as they should, and that at high frequencies the P wave ratio is lower than the L_g or SDHM ratios. The agreement between SDHM ratios and L_g could simply be due to the fact that the spectra computed by Borcherdt et al. (1967) which SDHM used were from a 12 second window which at PLMS and 10S and 20S included L_g. The various noise contamination problems discussed above would also tend to bias the spectral ratio high.

The fact that the P ratio is below the surface wave ratio suggests that the more steeply departing rays, which contribute to P, are less efficiently decoupled than are the more horizontally departing rays which go to make up the surface waves.

Healy et al. (1971) analyzed the SALMON-STERLING data in a slightly different manner than SDHM, computing spectra only of the first 5 seconds of data, thus eliminating problems with L_g. These spectral ratios were then fitted with a theoretical expression for the spectral ratio resulting from a pressure step, P, on a spherical cavity of radius a, with the two values of pressure and two values of radius adjusted to fit the data. The resulting pressure ratio was 4.15, and the equivalent elastic cavity was 29 meters for STERLING and 169 meters for SALMON. The low-frequency limit of this theoretical ratio is the ratio of a^3P, and the high frequency limit is aP. These limits are indicated on Figure 15 by the letter H and we see that they are in good agreement with our spectral ratio.

In Figure 16 we have cube-root-scaled the compressional ratio to several other yields, the requirement for validity is that a cavity be created at a depth of 830 meters in salt, and that then a shot of relative yield 0.38/5.3 be detonated at the cavity center. With this condition one may measure the amplitude from the large signal, and then divide by the observed spectral ratio to predict the observed amplitude from the decoupled explosion. Note

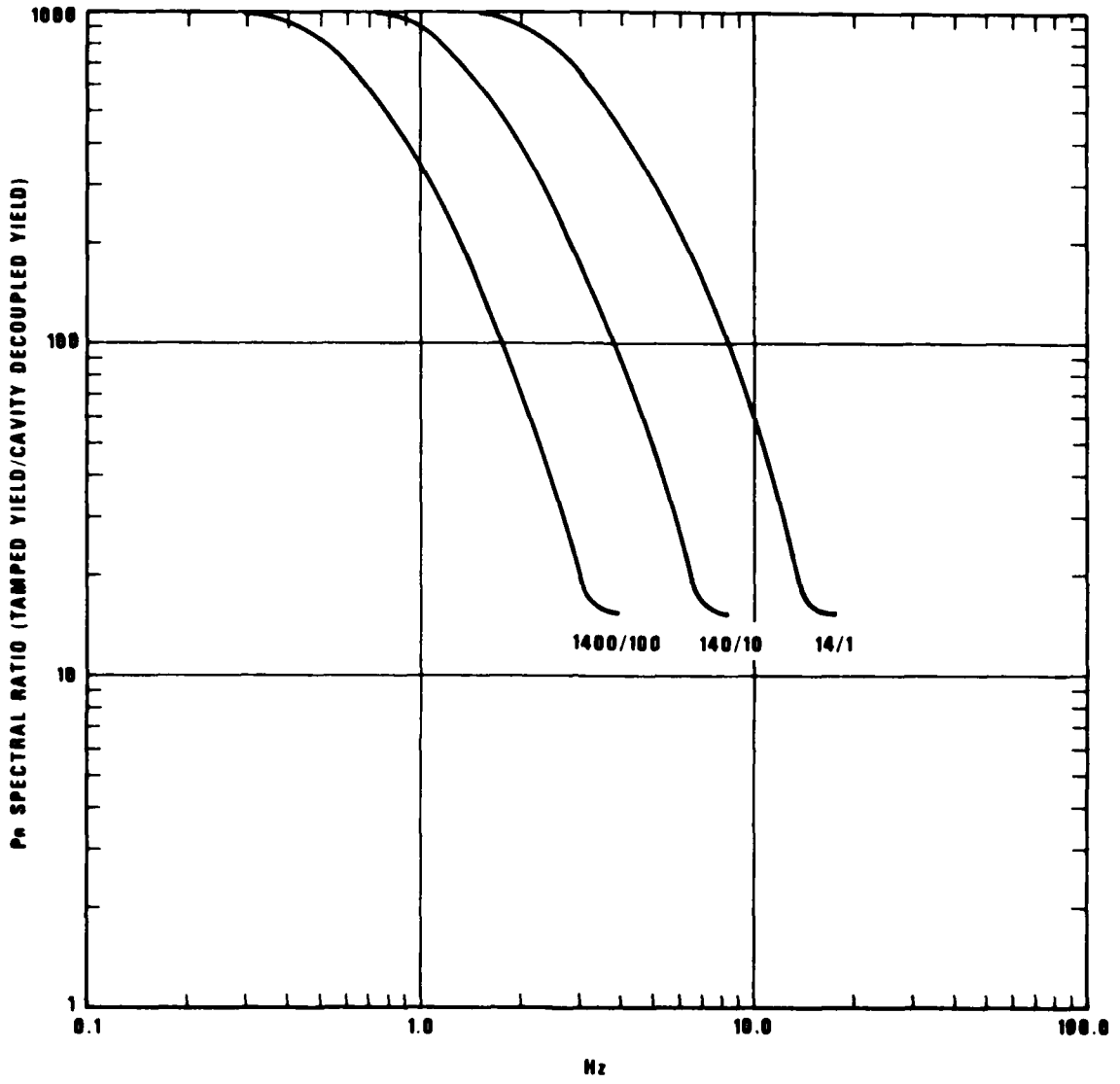

Figure 16. P_n SALMON/STERLING ratio from Figure 15 cube-root scaled at three different levels. To use graph select line by yield of explosion creating cavity, measure spectral amplitude at any desired frequency. Then division of this amplitude by the curve value at that frequency will give the expected amplitude of the decoupled shot. This expected signal amplitude may be compared to the ambient noise at the site.

that this approach by-passes the concept of the degree of decoupling, and of the reduced displacement potential.

In Figure 17 we see that there was poor agreement at high frequencies between the SDHM observed SALMON/STERLING spectral ratio and the theoretical calculations of Patterson (1966). However, note that the P ratio from Figure 15 would be in excellent agreement with a type of salt for STERLING between weakened salt I and very weak salt. Thus our observed ratio is in good agreement not only with the empirical-theoretical formulas of Healy et al. (1971) but also with the earlier theoretical calculations.

If it is desired to calculate the classical decoupling ratio as a function of frequency, then the ratio in Figure 15 must be multiplied by the spectral ratio of an 0.38 kiloton tamped shot to the 5.3 kt SALMON explosion.

The spectrum of 0.38 kt could be obtained from the spectrum of SALMON by cube-root scaling. However, to obtain the SALMON spectrum we are not, unfortunately, free to use the instrument corrected displacement spectrum at PLMS, JELA, etc., because such non-scalable effects as pP, absorption, and crustal interference complicate the picture. Thus, to obtain a SALMON source spectrum out to 25 Hz, we would be forced to use the free-field data.

Patterson. D. W. (1966). The calculation sensitivity of a model describing the response of a nuclear formed cavity: The STERLING event, Lawrence Radiation Lab. Report UCID-5125, Livermore, California.

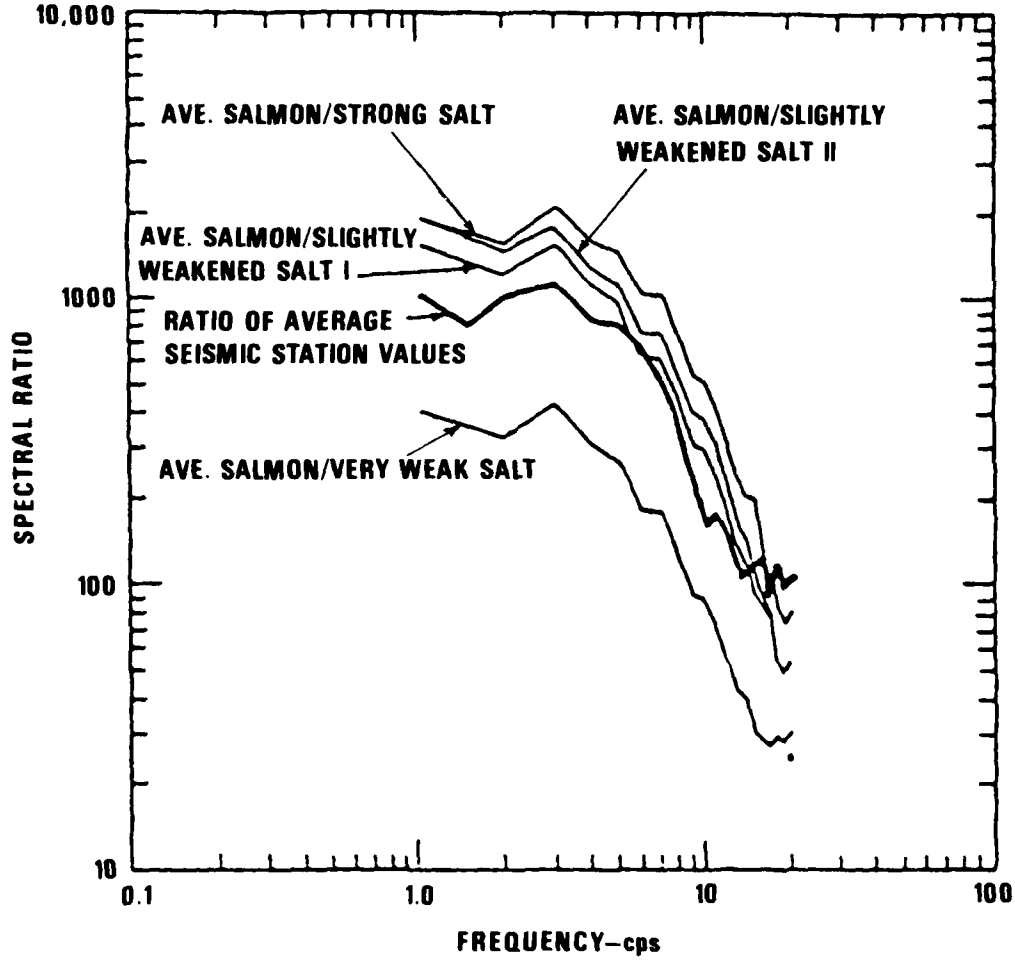

Figure 17. Theoretical spectral ratios for SALMON/STERLING from Patterson (1966) together with the observed spectral ratios plotted by Springer et al. (1968).

ANALYSIS OF SALMON/(STERLING NOISE) SPECTRAL RATIO AT JELA,(EUAL, EU2AL)

In the preceding section we have seen data from stations at 27 and 112 km from STERLING and SALMON. The next closest stations for which we have data are those at JELA and (EUAL, EU2AL) which were at distances of 243.0 and (242.2, 242.9) kilometers, respectively (see Figure 18). At neither of these stations was there clearly detected a signal from STERLING; however, we shall see that some useful limits on the spectral ratio may be obtained from the (SALMON signal)/(STERLING noise) ratio.

Figures 19 and 20 show the SALMON data at JELA and EUAL. (We note that for the initial 7 seconds the vertical component is much larger than the radial or transverse, showing that the signal is arriving at near vertical incidence. This suggests that if a crustal model could be developed for source and receiver, then its effects might be taken out of the data and a SALMON source spectrum recovered, considering, as we shall see, that valid data extends well above 10 Hz on the analog tape.)

Figure 21 shows the STERLING P window at JELA. From Figure 19 we deduce that the expected arrival time for Figure 21 would be 12:15:37.2, and that the maximum detectability would be on the radial channel between 12:15:47 and 12:16:05. In fact, inspection of the STERLING radial trace does reveal a suggestion of a signal between 12:15:58 and 12:16:05.

Concentrating, however, on the vertical trace we see in Figure 22 the noise and signal for SALMON and the corresponding spectra. (Note the remarkable parallelism between the noise and signal spectra. That this is not an artifact of the digital data processing may be seen by the fact that the time domain noise (system noise) is similar in character to the SALMON signal itself.

Also in Figure 22 may be seen the STERLING P-window noise taken from the spectrum in Figure 23. The interval between the SALMON signal spectrum and the STERLING noise, is the source of the arrows plotted in Figure 15. In that figure it is noteworthy that the arrow at 2.6 Hz presses just below the observed ratio of 1000, a fact in good agreement with the marginal detection on the radial trace in Figure 21.

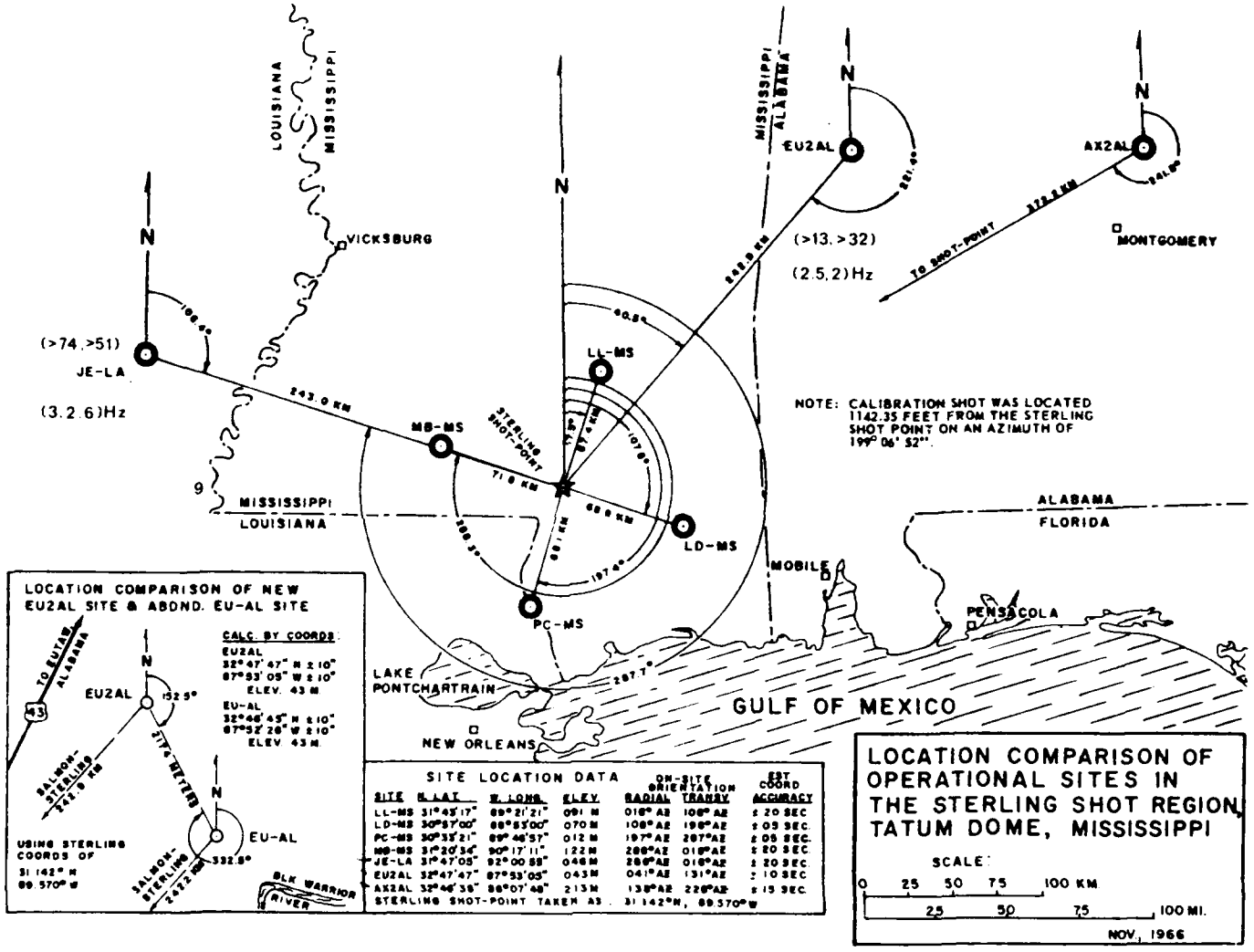

Figure 18. Time domain decoupling ratio limits for (P, Lg). Maximum amplitudes were picked for SALMON and then the maximum noise pulse of the same frequency was picked within 5 seconds of the expected arrival time for STERLING. The ratios were scaled by the ratio of the yields before plotting.

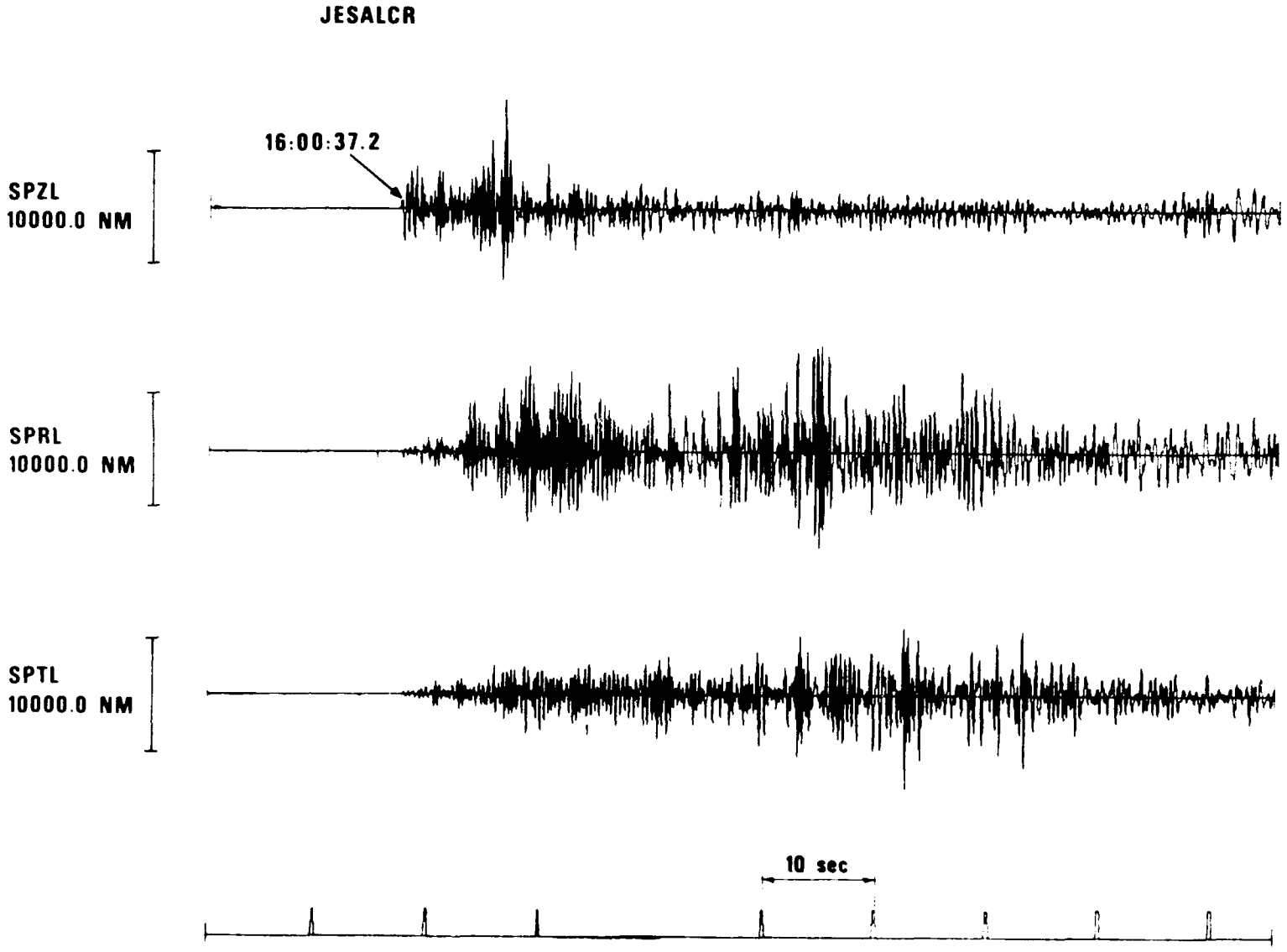

Figure 19. Three rotated components of SALMON as seen at station JELA.

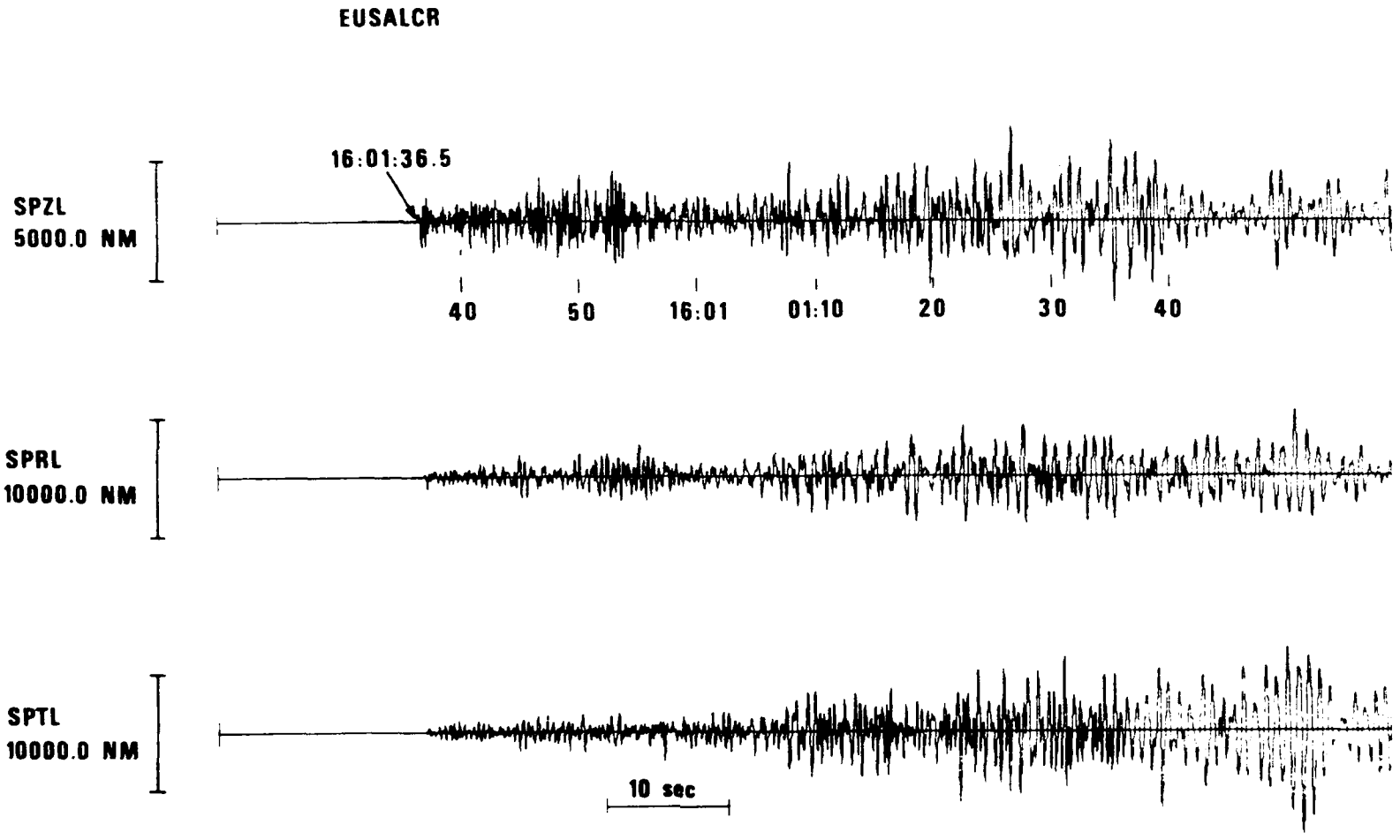

Figure 20. Three rotated components of SALMON as seen at station EUAL.

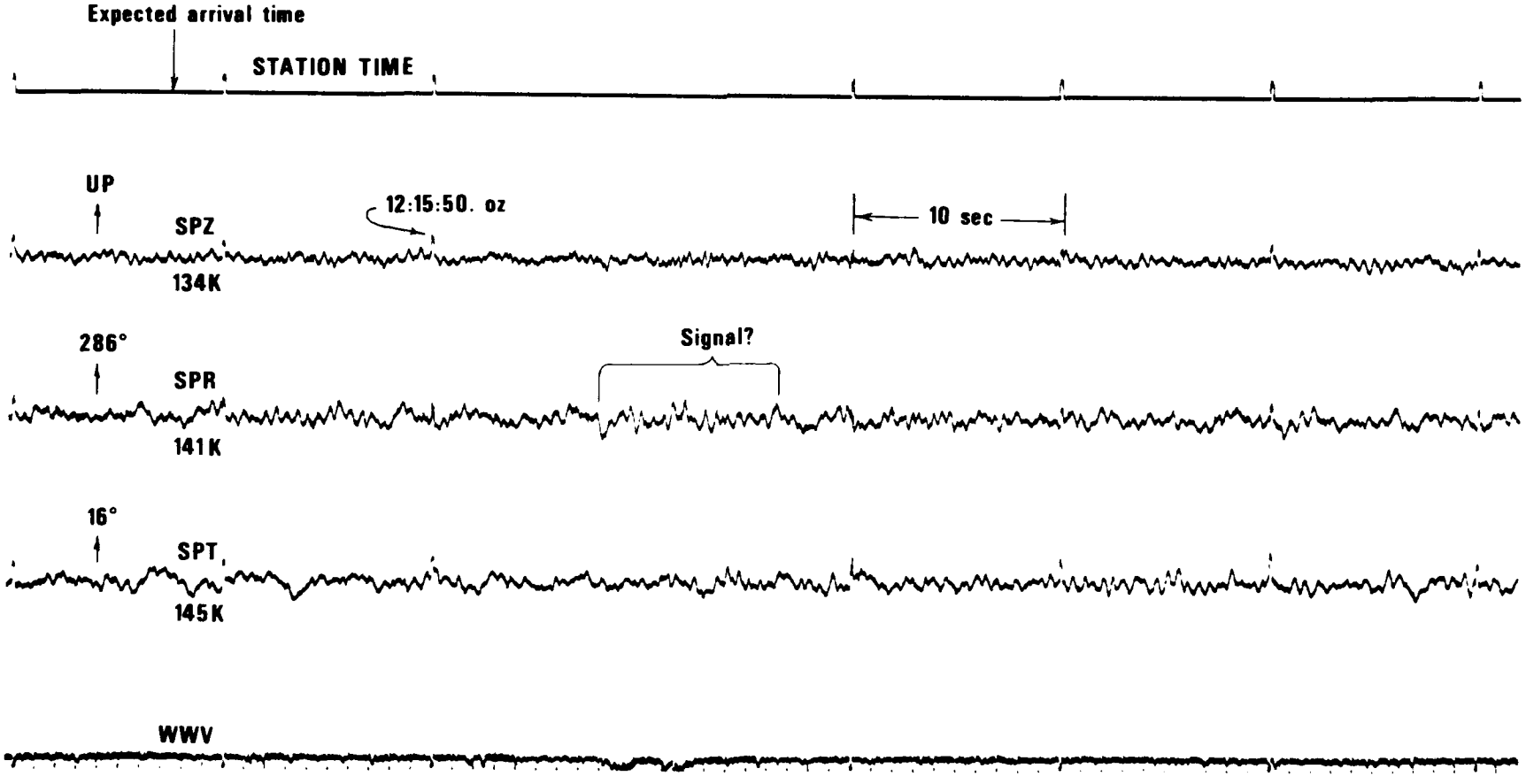

Figure 21. Three rotated components of STERLING as seen at station JELA. From Geotech Technical Note TN-67-5.

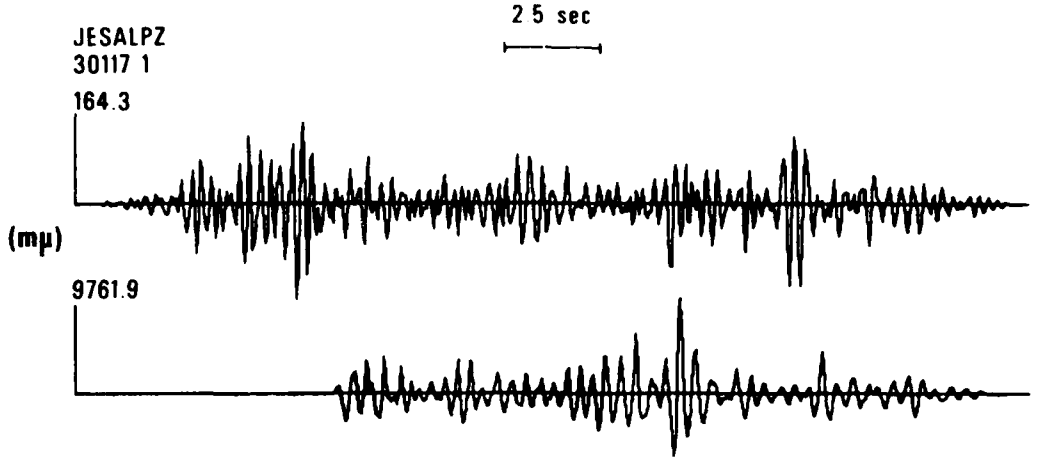

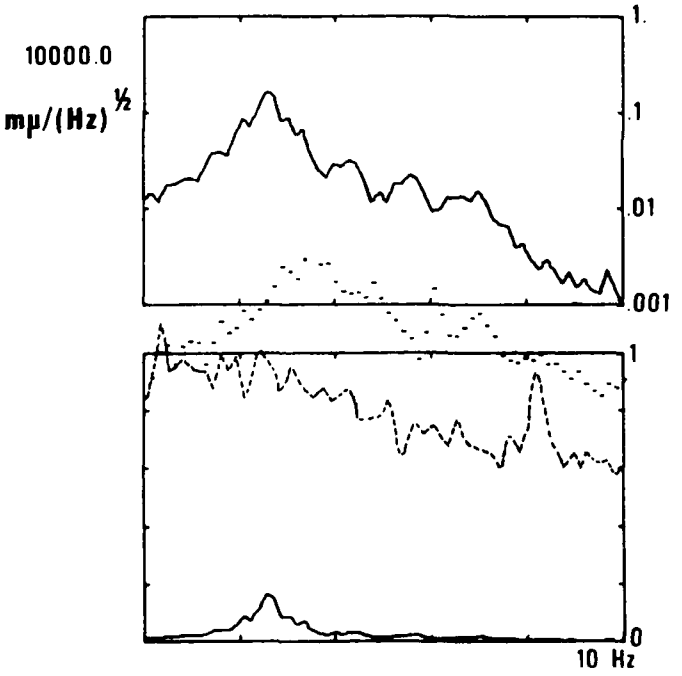

Figure 22. P-wave signal and noise of SALMON as seen at station JELA. Vertical component. Amplitude in mμ. Spectrum is square root of the power spectrum. Middle dotted line is noise spectrum. Lower dashed line is noise from corresponding signal window of STERLING.

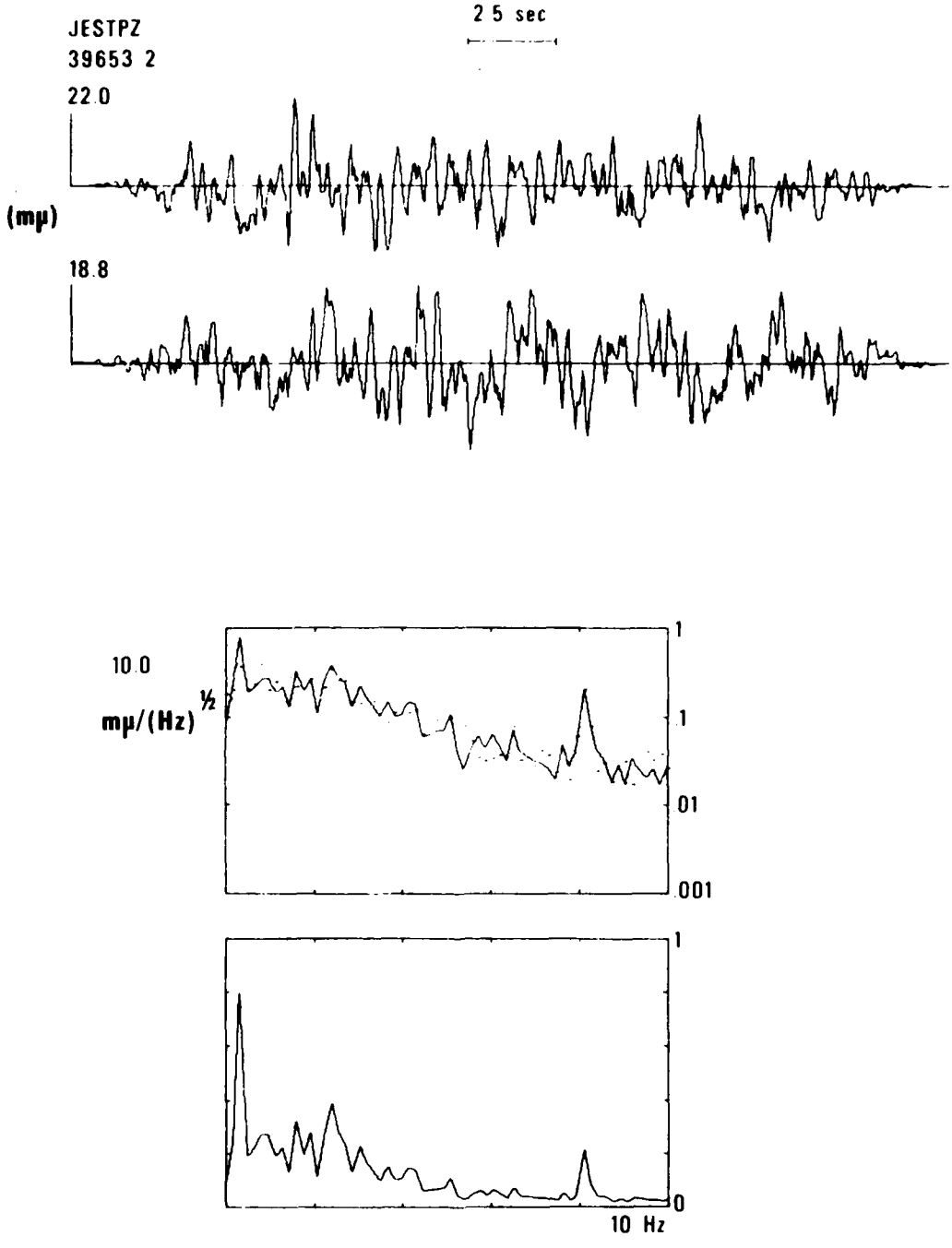

Figure 23. P-wave signal window and noise window of STERLING as seen at station ILA. Vertical component. Amplitude in mμ. Spectrum is square root of the power spectrum.

Figures 24 and 25 give the SALMON L_g signal spectrum and the corresponding window for STERLING. We note that the SALMON L_g is more sustained than the P wave, but at about the same amplitude, so that we are not surprised in view of the marginal detection status at JELA to see that the L_g window for STERLING (Figure 25) has a higher amplitude than the P window (Figure 23); the signal may well be hidden in the noise. However, E. Smart has attempted to determine the back azimuth to STERLING using his L_g processor (Smart, 1977) on this window. The results were inconclusive in that, although a correct back azimuth was determined, runs of the program in the time window before the signal arrival also gave the same azimuth, suggesting that the ambient noise at the time had the nature of a signal propagating from the direction of the shot point.

Were a limit to be determined from Figure 24, its maximum would be about the same as that determined from Figure 22; it is a factor of ~ 1000 at 2.9 Hz. If the L_g is actually present in this window, then this is practically a true signal ratio, and would fit just at the appropriate place with respect to the L_g curve in Figure 15.

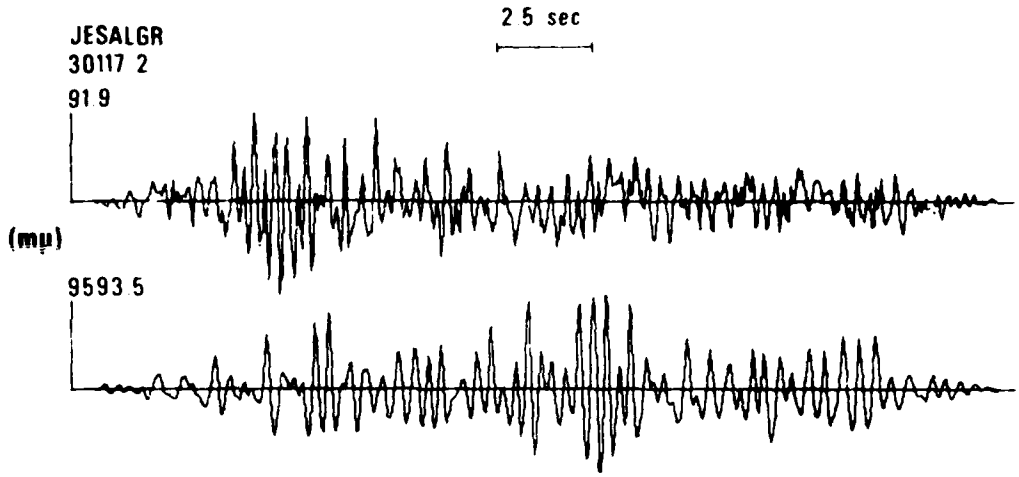

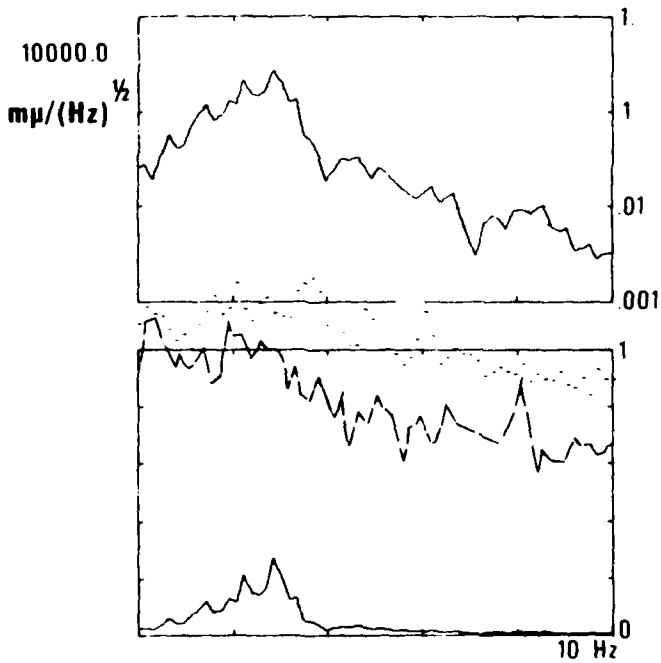

Figure 24. L$_g$-wave signal and noise of SALMON as seen at station JELA. Vertical component. Amplitude in mμ. Spectrum is square root of the power spectrum. Middle dotted line is noise spectrum. Lower dashed line is noise from corresponding signal window of STERLING.

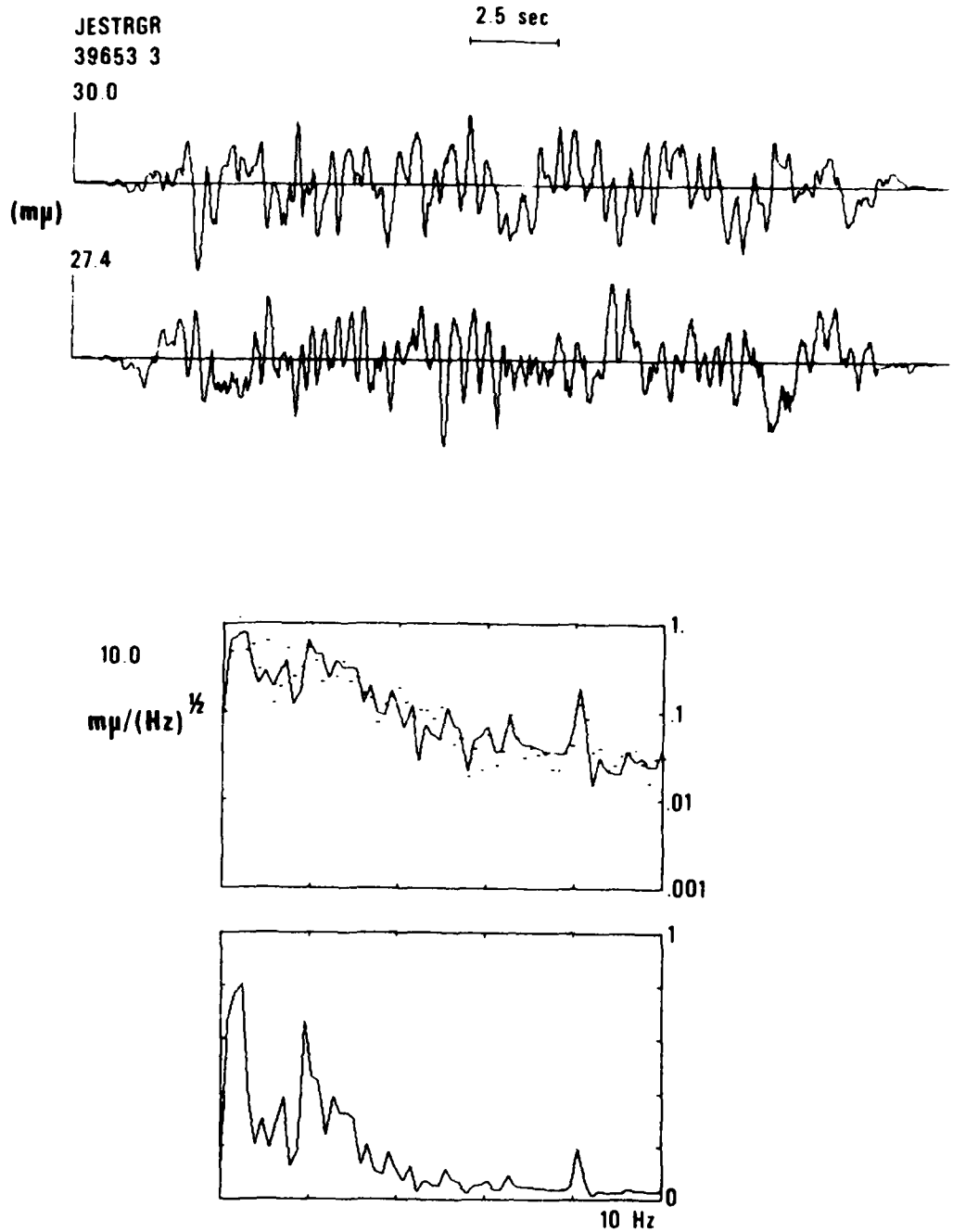

Figure 25. L_g-wave signal window and noise window of STERLING as seen at station JELA. Vertical component. Amplitude in mμ. Spectrum is square root of the power spectrum.

ANALYSIS OF POSSIBLE "ANOMALIES" IN STERLING/STERLING CAL AMPLITUDE RATIOS

Some controversy has arisen over the variation at different stations in apparent decoupling between STERLING and the "STERLING CAL," a high-explosive shot detonated 1142 feet from the STERLING shot and at the same depth. I feel that such variations can be explained by the difference in shot points, but herewith we do present the data. Figure 26 from TN-67-5 shows the STERLING signal at LDMS (all station locations may be seen in Figure 18), and Figure 19 shows the STERLING CAL signal at the same station. The amplitude ratio near 2 km/sec on the radial component at 1.4 Hz is 5.0. In Figure 28 this number is plotted together with the corresponding ratios at the other three LRSM stations at a distance of 70 km. We see that there is substantial variation in the ratios, which might be due to an azimuthal variation in decoupling, but which may be more economically explained as difference in propagation due to the two shot points being in different locations.

The STERLING CAL shot was 2 tons of high-explosive. If we assume that one ton of high explosive is equivalent to one ton of nuclear explosive, and assume no spectral scaling, (this would be valid if the corner frequency were > 5 Hz for both events) then from the time domain measurements we may compute the apparent decoupling ratios in Figure 29. The logarithmic average of these should average out propagation fluctuations to some degree and is > 76, in reasonable agreement with the numbers derived by SDHM.

Figure 30 gives the amplitude ratios which could be determined using the P phase on the vertical component. Only limits could be obtained.

An analysis similar to that performed for the STERLING CAL has been performed using plots from the Geotech Technical Report (Johns, 1970) for the event HUMID WATERS which was detonated precisely at the STERLING shot point. The results of these two analyses are summarized in Figure 31. We see that the observed measurements for the STERLING/STERLING CAL scatter much more than

Johns, Frank H. (1970). Preliminary report on long range seismic measurements participation in project MIRACLE PLAY - HUMID WATERS, TR-70-16, Teledyne Geotech, Garland, Texas.

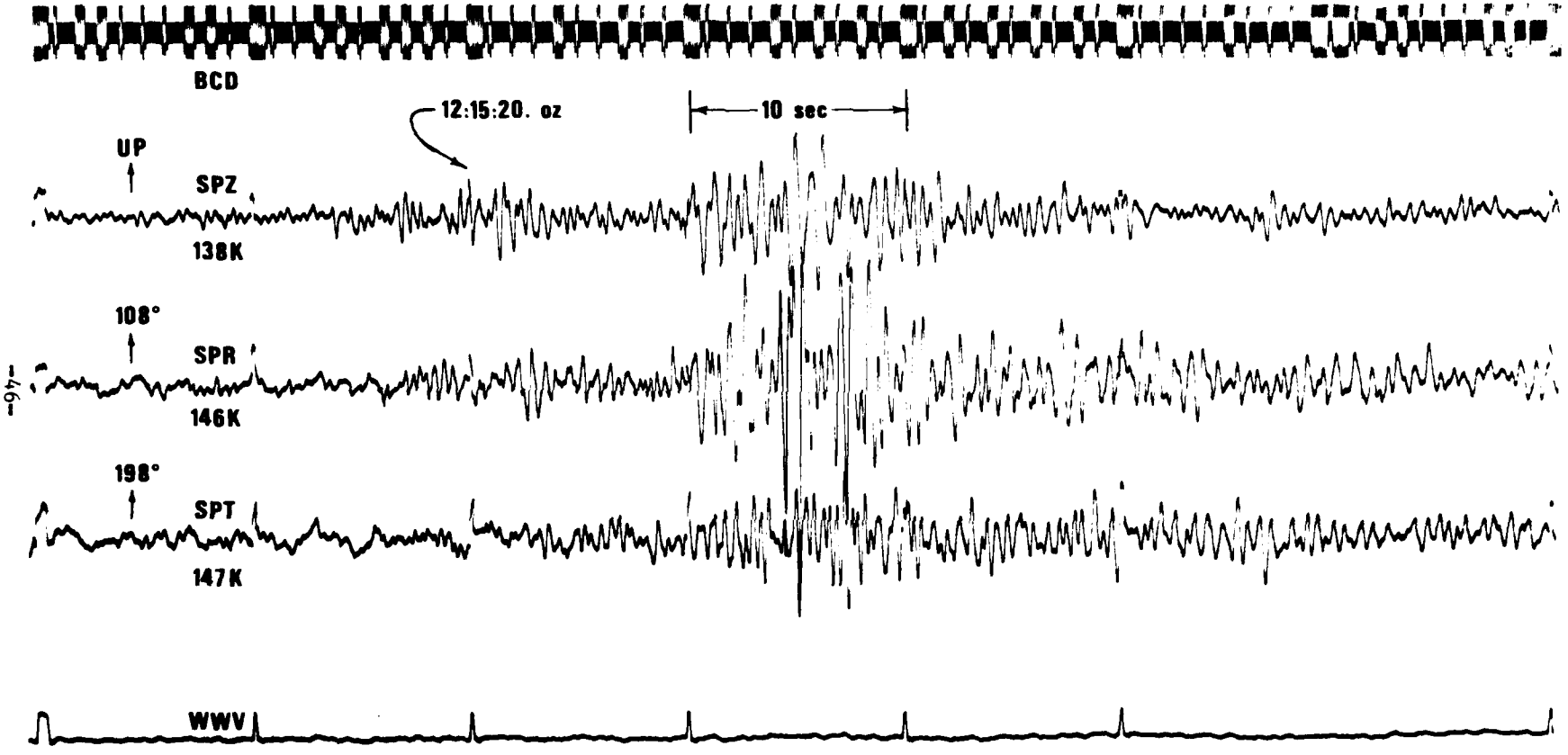

Figure 26. Three rotated components of STERLING as seen at station LDMS. From Geotech Technical Note TN-67-5.

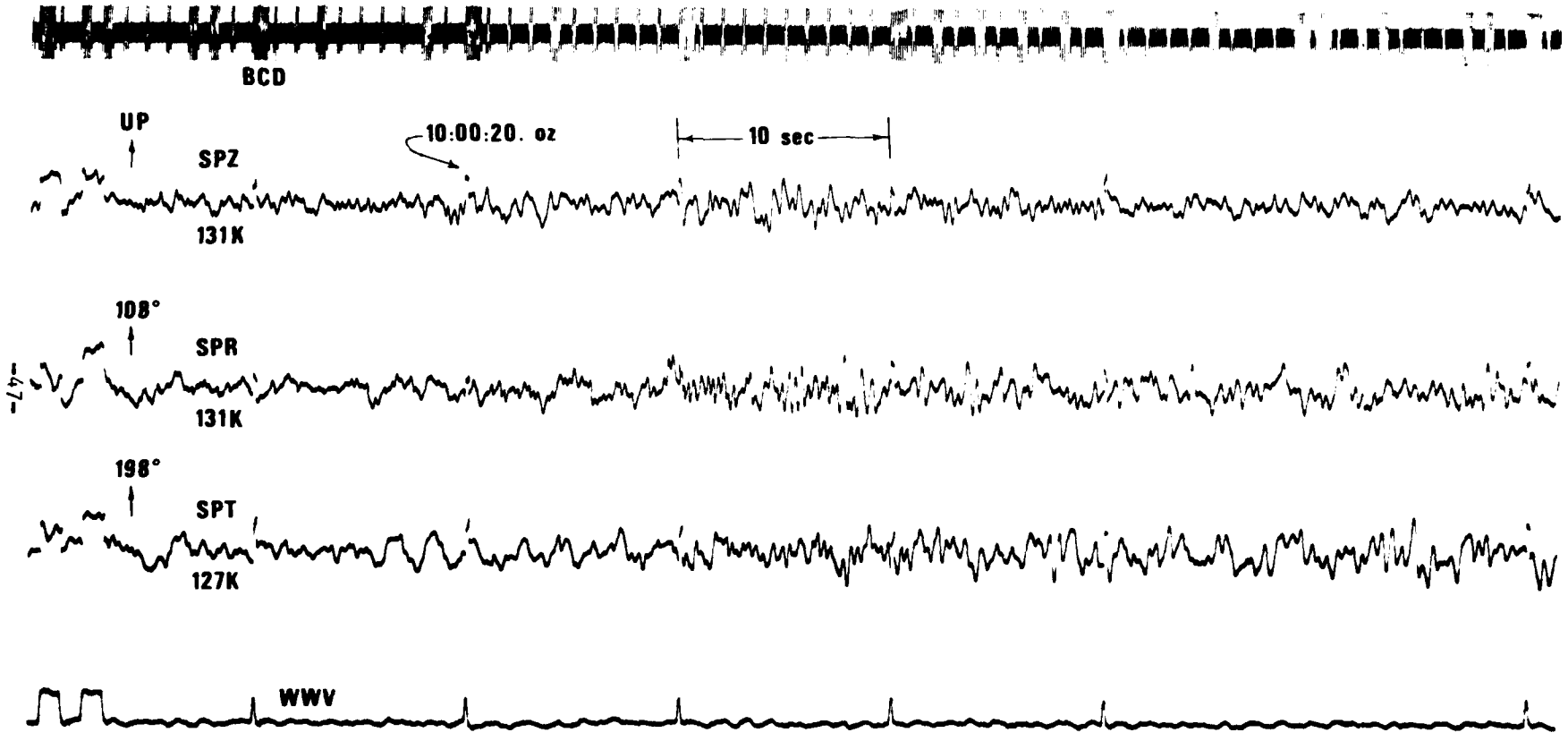

Figure 27. Three rotated components of STERLING CAL as seen at station LDMS. From Geotech Technical Note TN-67-5.

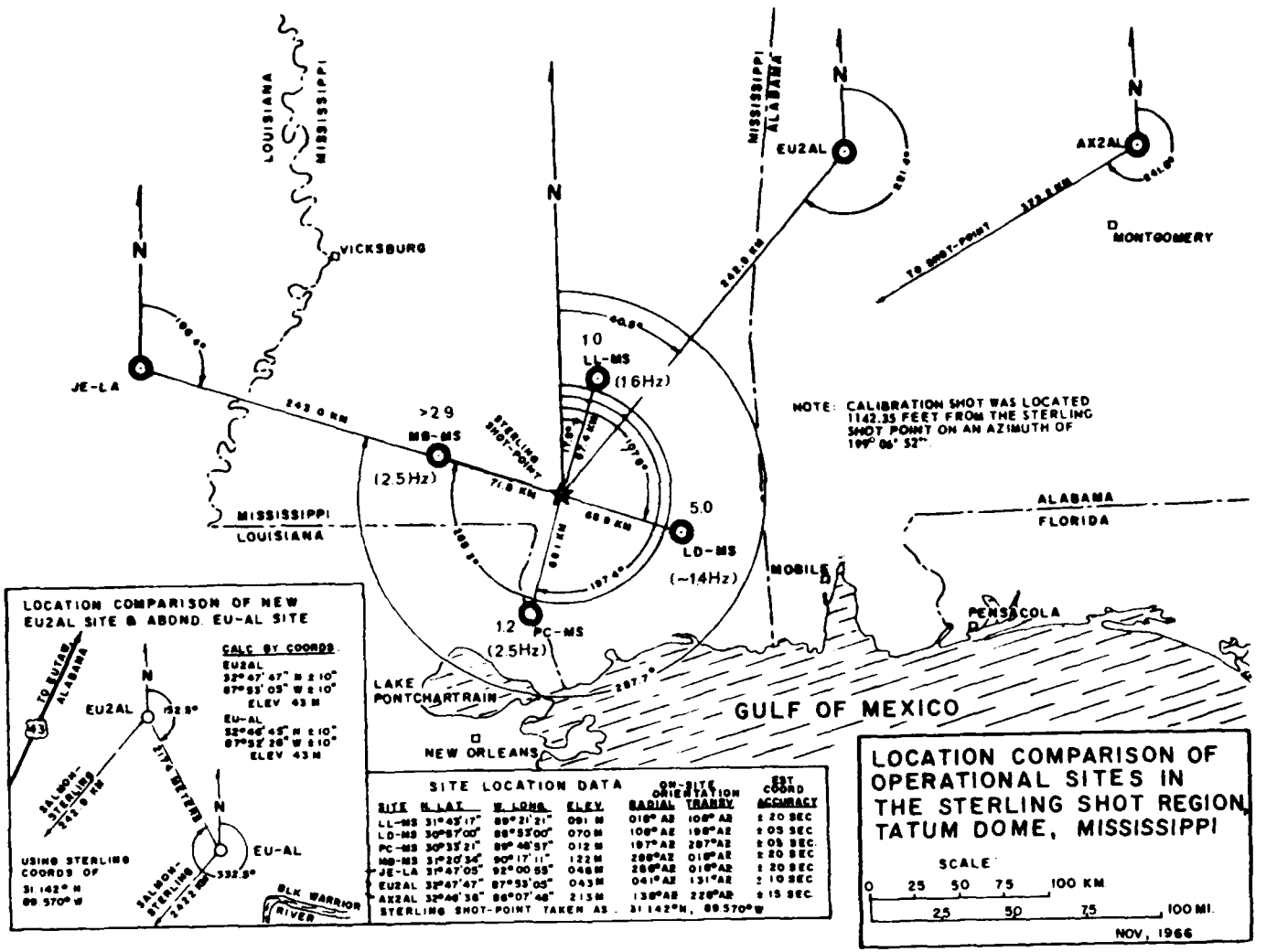

Figure 28. Amplitude ratio of maximum of radial component of STERLING to maximum of STERLING CAL within 5 seconds of the expected arrival. Measurements made at identical periods for both events.

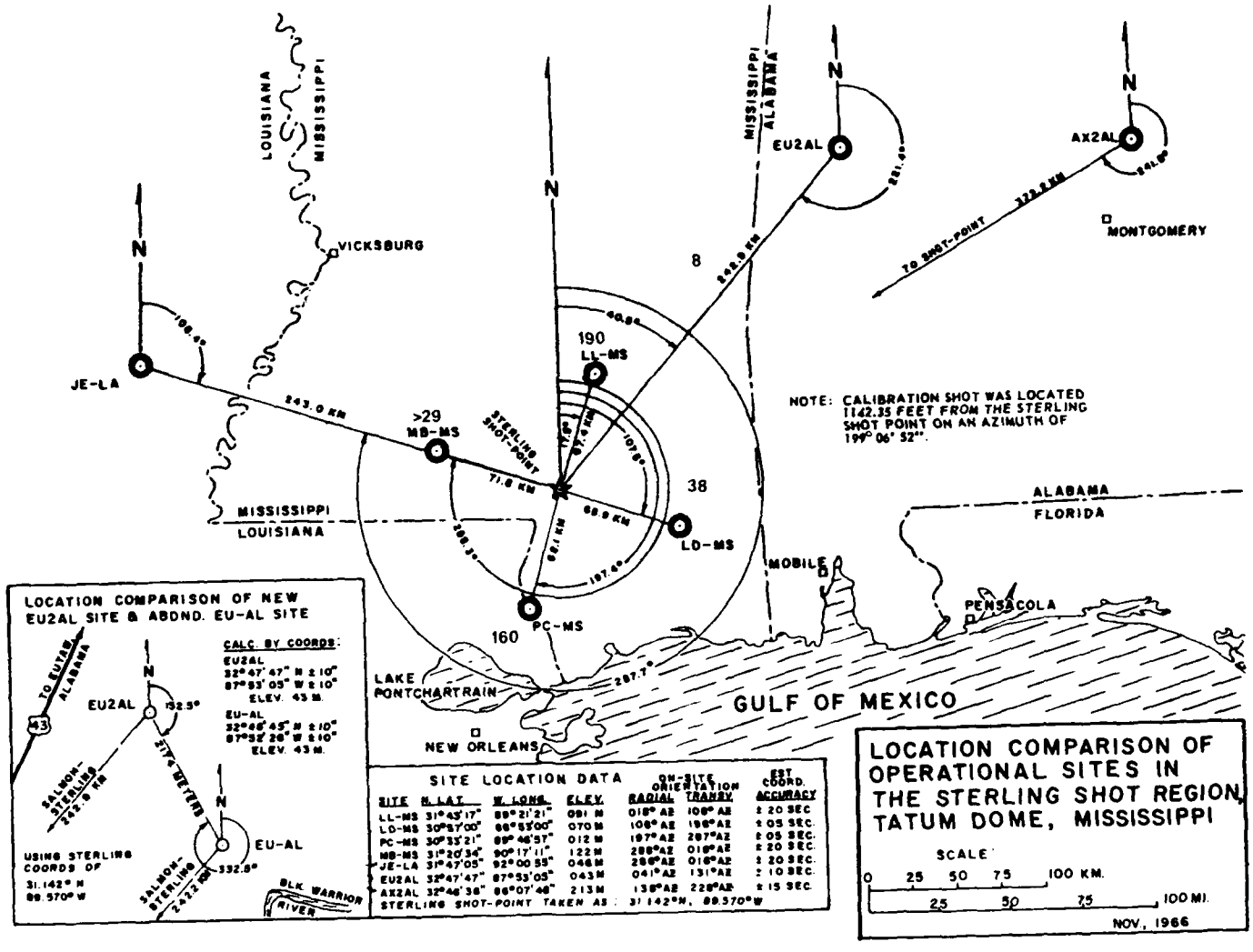

Figure 29. Ratios from Figure 28 scaled by yields; at these frequencies the result is the decoupling factor.

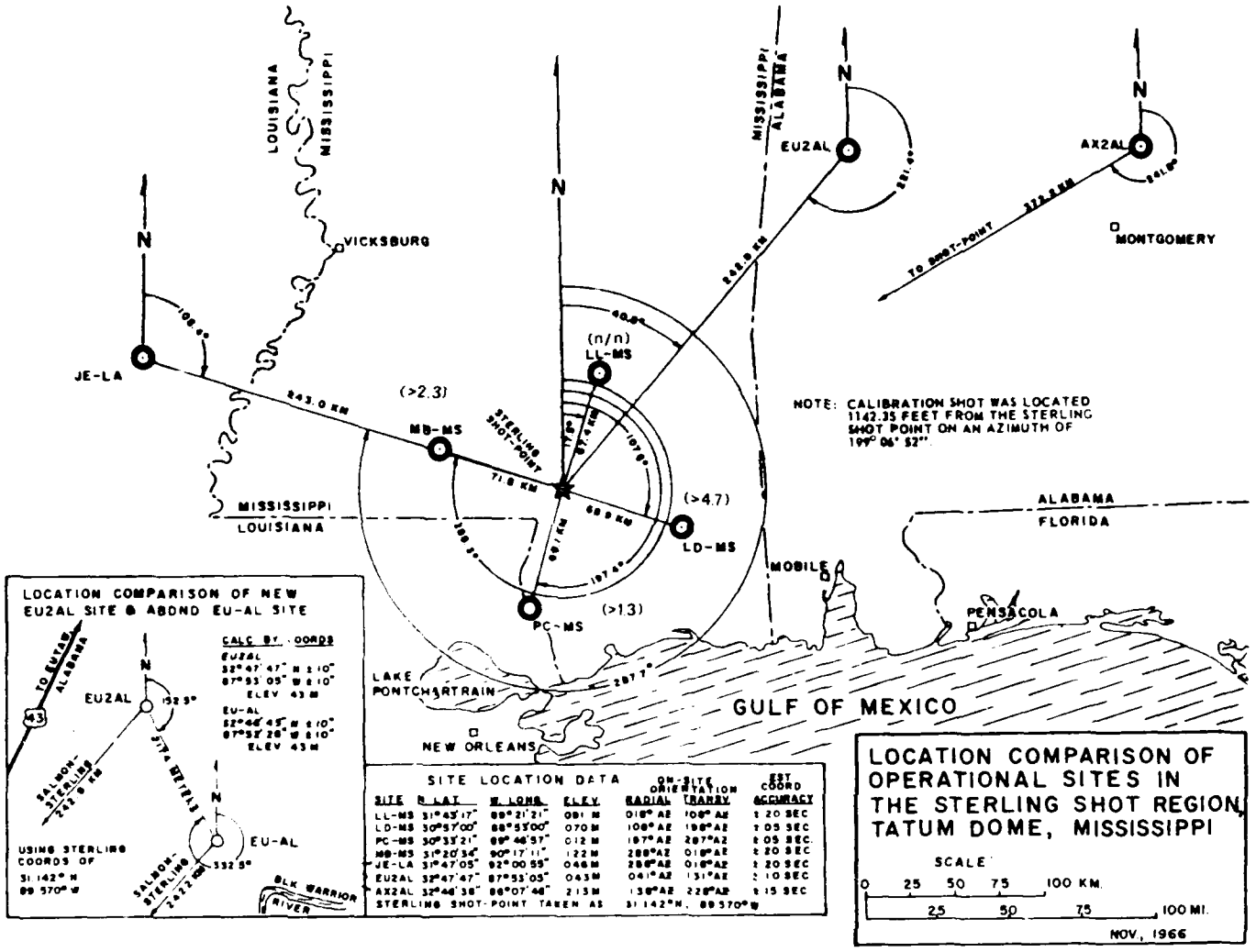

Figure 30. Amplitude ratio of maximum of vertical component of STERLING to maximum of the STERLING CAL in the first 10 seconds of the expected arrival. Measurements made at the same period for both events.

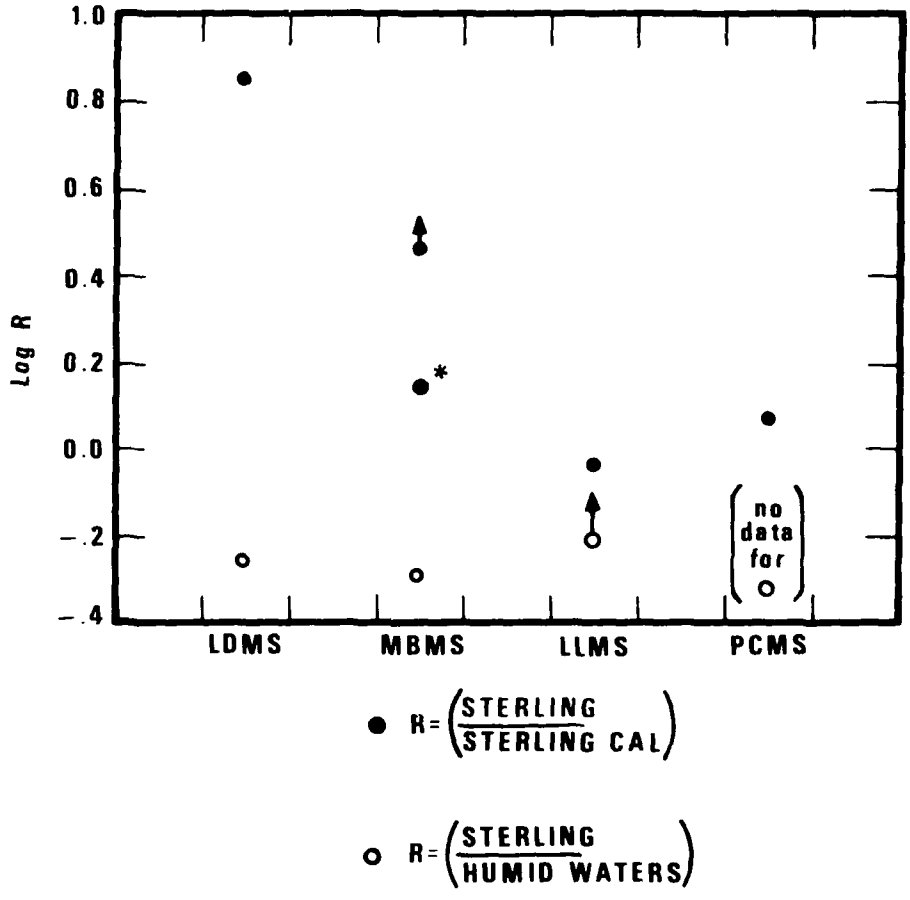

Figure 31. Time domain amplitude ratios from the radial components of STERLING, STERLING CAL and HUMID WATERS. Amplitudes measured within 5 seconds of the STERLING maximum except for the point marked with the asterisk where the maximum for the STERLING CAL was later than the 5 second window.

do the observed measurements for STERLING/HUMID WATERS. Unfortunately, however, LDMS is the only station for which, within 5 seconds travel time of the maximum motion near 2 km/sec for SALMON, there is also a clear signal for STERLING CAL and for HUMID WATERS. If, however, we use the maximum motion anywhere in the signal, it is possible to get a signal for HUMID WATERS AT MBMS, and to explicitly see the greater range in the CAL data as compared to HUMID WATERS. The necessity to look in a different time window for the maximum signal reflects the fact that the STERLING CAL signal is different in shape from that of STERLING or of HUMID WATERS, which again reflects the fact that the shots are detonated at different locations.

SDHM have also pointed this out. Figure 6 shows that when filtered in the band 1-2 Hz, the band of interest in this discussion, then SALMON and STERLING at the same shot point have nearly identical waveforms which are quite different from that of STERLING CAL (HE STERLING).

Figure 32-35 are presented with the thought that future workers may find them of some use. Here we have the noise and signal windows and corresponding spectra for STERLING for the 2 km/second pulse at the four innermost stations in Figure 11. The dashed line in each figure is the signal spectrum of the STERLING CAL for the frequency range in which S/N > 2. We see in general that in the spectral domain we see the same amplitude ratio as in the time domain. There is some indication in the LDMS data that the spectral ratio is greater at 2 Hz than at 4 Hz.

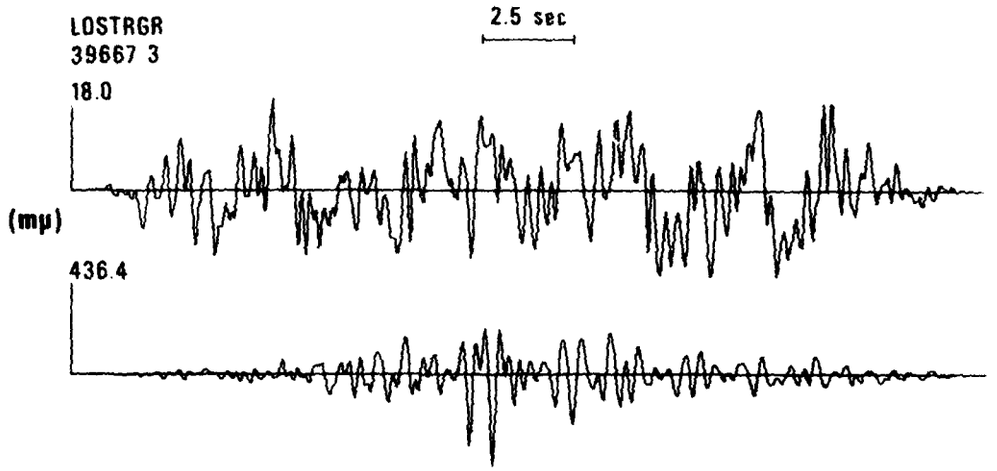

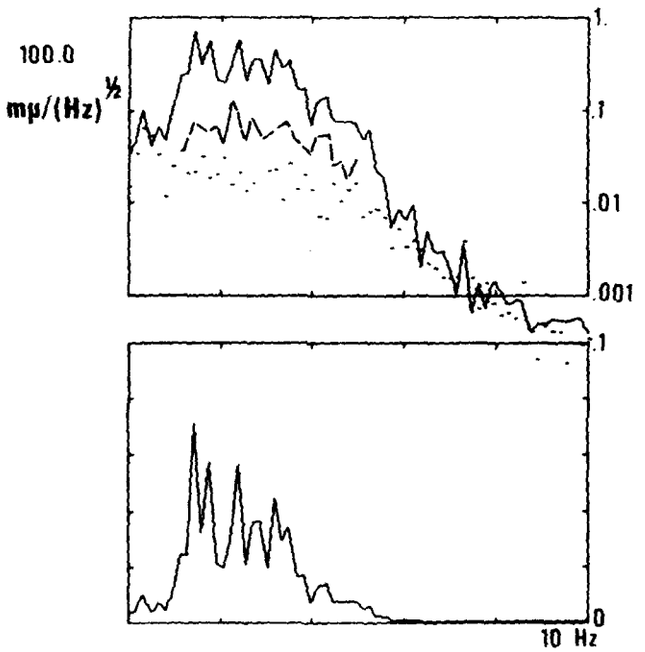

Figure 32. Noise and signal amplitude and spectra from radial component of STERLING at LDMS in the time window surrounding 2 km/sec. The dashed line represents the corresponding signal spectrum from STERLING CAL where the S/N is greater than 2.0.

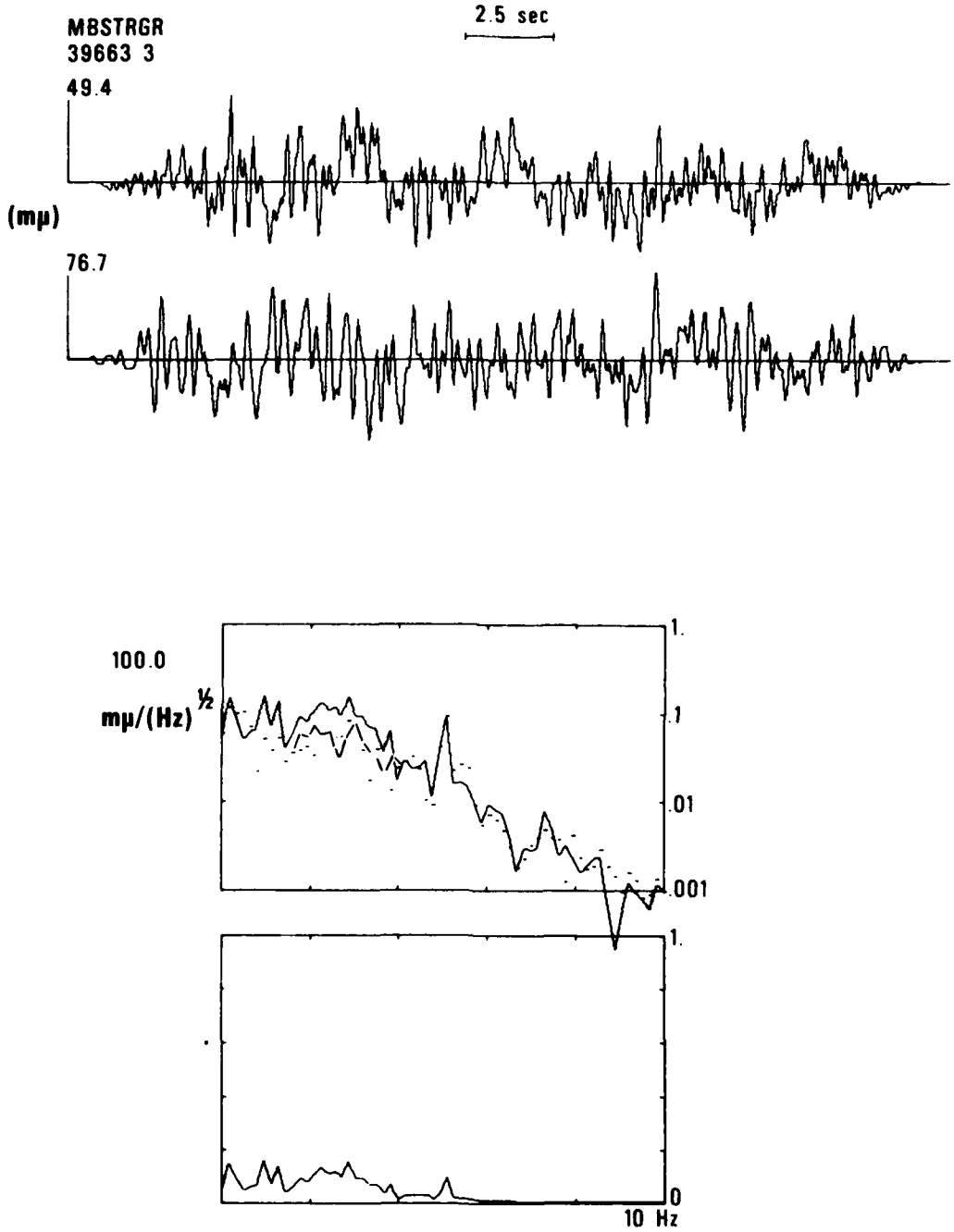

Figure 33. Noise and signal amplitude and spectra from radial component of STERLING at MBMS in the time window surrounding 2 km/sec. The dashed line represents the corresponding signal spectrum from STERLING CAL where the S/N is greater than 2.0.

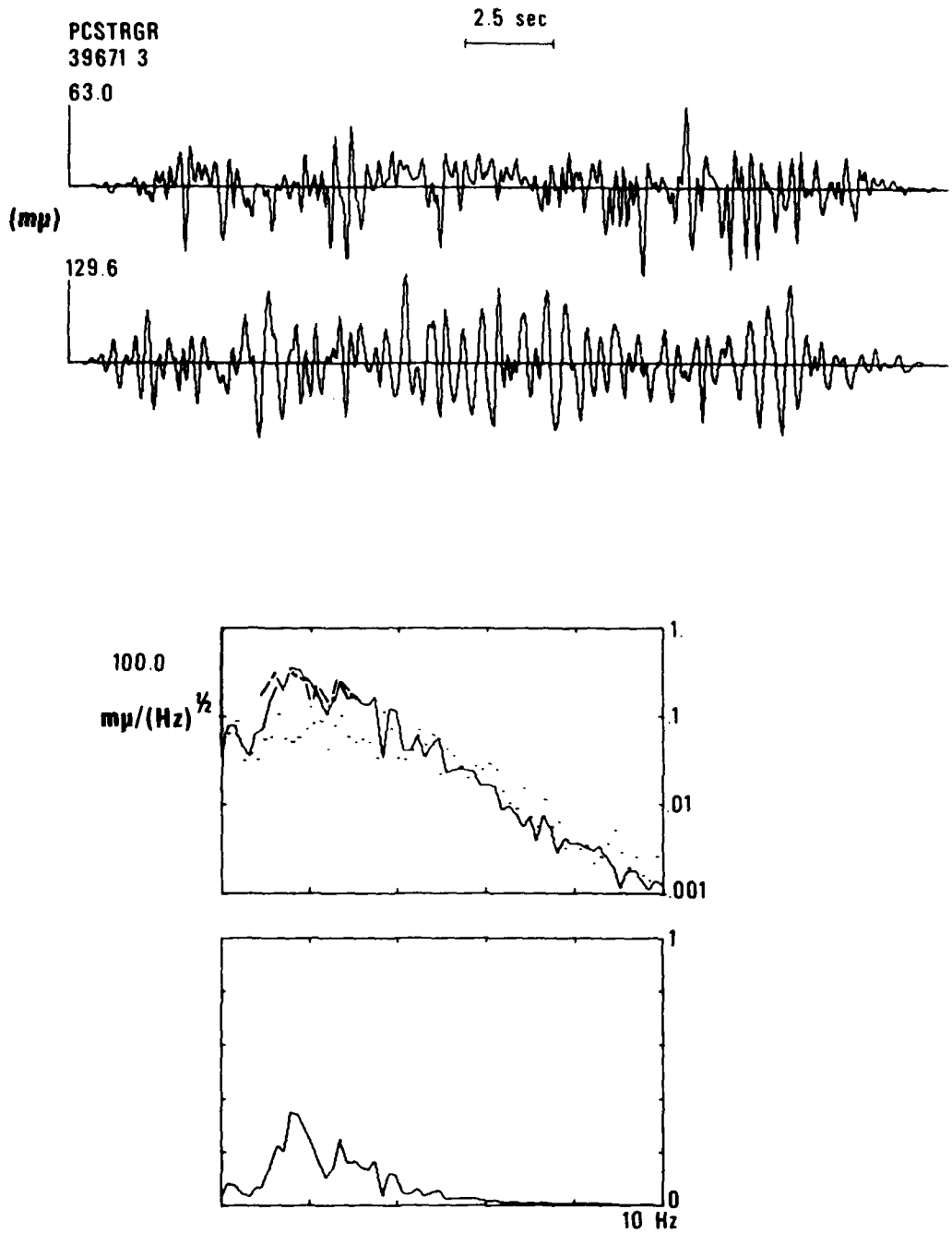

Figure 34. Noise and signal amplitude and spectra from radial component of STERLING at PCMS in the time window surrounding 2 km/sec. The dashed line represents the corresponding signal spectrum from STERLING CAL where the S/N is greater than 2.0.

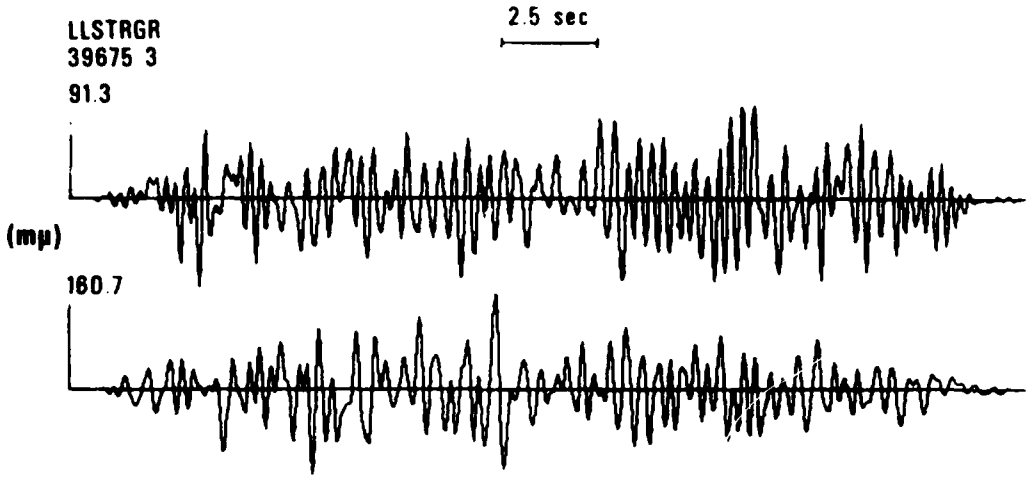

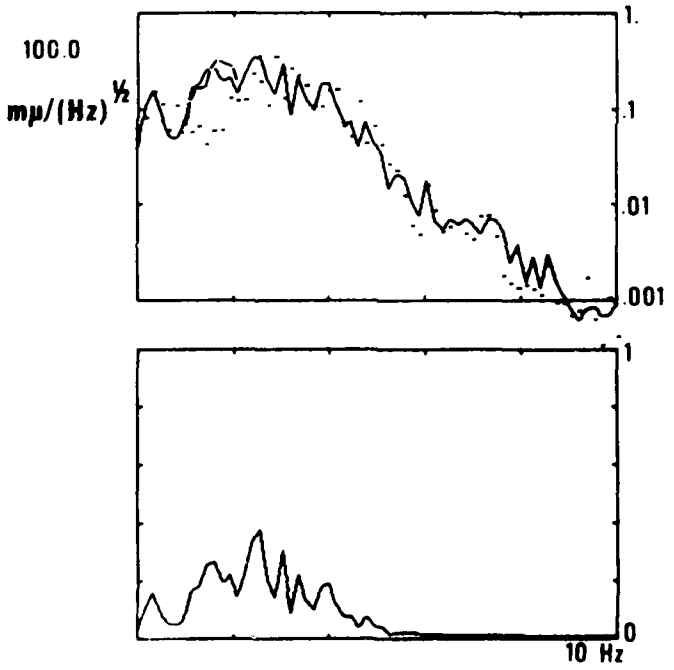

Figure 35. Noise and signal amplitude and spectra from radial component of STERLING at LLMS in the time window surrounding 2 km/sec. The dashed line represents the corresponding signal spectrum from STERLING CAL where the S/N is greater than 2.0.

SUMMARY AND DISCUSSION OF POSSIBLE FURTHER RESEARCH

Analysis of data from PLMS and RLMS has verified the low-frequency SALMON/STERLING spectral limits of SDHM and of Healy et al. (1971). For high frequencies (25 Hz) the spectral ratio declines to a value near 17 as contrasted to the value of 100 reported by SDHM but in agreement with the trends predicted by code calculations at high frequency by Patterson (1966), and in agreement with the high-frequency limit of the ratio of two model spectra fitted to the data by Healy et al. (1971). When cube-root scaled to larger yields, this result predicts that it will be easier to detect the high frequencies from P waves from decoupled explosions than has been thought possible heretofore.

For surface waves the decoupling at high frequencies is the same as that found by SDHM. Springer used spectra computed by Borcherdt et al. (1967) and by USC&GS workers so that to some extent this is an accidental result because it would appear that the high frequency estimates of Borcherdt et al. (1967) were badly biased by spikes and system noise, in addition to being biased by the L_g contained in their 12 second windows at stations PLMS. We do not know the size of the window used by USC&GS for their spectral calculations at 10S and 20S, but if they also used 12 seconds the spectral ratios there would also be biased toward the L_g ratio.

The variation in the STERLING/STERLING HE spectra can be explained by the variation in shot point between these two explosions, and not necessarily by a variation in decoupling as a function of azimuth. This is shown most clearly by comparison with the more constant ratio STERLING/HUMID WATERS, because HUMID WATERS was detonated in the STERLING cavity.

Future work should include:

- Analyze data from stations 10S and 20S to confirm if possible the high-frequency results which rest, at present, on the first 2.5 seconds of SALMON data of channel 1 at PLMS.

- Analyze as much of the data as possible from the stations in Figures 1 and 18 to determine amplitude-distance curves as a function of distance at these close ranges.

- From an accumulated comprehensive data base to 250 km, extend the study of the growth of the transverse/radial component of motion as a function of distance to include frequency and greater distances, (see the previous work in Figure 6 of Werth and Randolph (1966)). That figure shows that the peak raw particle radial to transverse velocity ratio for SALMON varied from 10:1 at 1 km to about 1:1 at 30 km. This is a unique data set to examine for growth of transverse motion which is of importance for discrimination.

- Investigate the use of SALMON data at JELA, EUAL, and possibly CPO, for determination of the high-frequency SALMON RDP. Crustal and absorption effects would have to be estimated and eliminated; however, it may be possible to do this, yielding a truly "linear regime" RDP. The crustal effects on the path to PLMS might well be too difficult to untangle.

ACKNOWLEDGEMENTS

This work was supported by the Advanced Research Projects Agency of the U. S. Department of Defense under Contract F08606-78-C-0007 as administered by the Air Force Technical Applications Center.

REFERENCES

Blandford, R. R. (1976). Experimental determination of scaling laws for contained and cratering explosions, SDAC-TR-76-3, Teledyne Geotech, AD A030 765.

Borcherdt, R. D., J. H. Healy, W. H. Jackson, and D. H. Warren (1967). Seismic Measurements of Explosions in the Tatum salt dome, Mississippi, Technical Letter Number 48, United States Geological Survey.

Healy, J. H., C. King, and M. E. O'Neill (1971). Source parameters of the SALMON and STERLING nuclear explosions from seismic measurements, J. Geophys. Res., 76, 3344-3355.

Johns, Frank H. (1970). Preliminary report on long range seismic measurements participation in project MIRACLE PLAY-HUMID WATERS, TR-70-16, Teledyne Geotech, Garland, Texas.

Jordan, J. N., W. V. Mickey, W. Helterbran, and D. M. Clark (1966). Travel times and amplitudes from the SALMON explosion, J. Geophys. Res., 71, 3469-3482.

Murphy, J. R. (1969). Discussion of paper by D. Springer, M. Denny, J. Healy, and W. Mickey, The STERLING experiment: decoupling of seismic waves by shot-generated cavity, J. Geophys. Res., 74, 6714-6718.

Patterson, D. W. (1966). The calculation sensitivity of a model describing the response of a nuclear formed cavity: The STERLING event, Lawrence Radiation Lab., Report UCID-5125, Livermore, California.

Smart, E. (1977). A three-component single-station maximum-likelihood signal processor, SDAC-TR-77-14, Teledyne Geotech, Alexandria, Virginia.

Springer, D., M. Denny, J. Healy, and W. Mickey (1968). The STERLING experimentL decoupling of seismic waves by a shot-generated cavity, J. Geophys. Res., 73, 5995-6011.

Wolfe, R., (1967). Quarterly report no. 4, proj. 9714. Teledyne Geotech, Garland, Texas.